PROJECT COMPASS-II

STUDIES OF THE NUCLEON AND HADRON STRUCTURE AT CERN
THEME 02-0-1085-2009/2019

EXTENTION FOR 2017-2019

PARTICIPATING INSTITUTES AND INTERNATIONAL ORGANIZATIONS:

CERN:CERN
CZECH REPUBLIC: Charles University in Prague, Faculty of Mathematics and Physics
Czech Technical University in Prague, Institute of Scientific Instruments (Brno),
Technical University in Liberec
FRANCE: IRFU, CEA, Université Paris-Saclay
GERMANY: Universität Bochum-Institut für Experimentalphysik, Universität Bonn,
Helmholtz-Institut für Strahlen- und Kernphysik, Universität Bonn- Physikalisches Institut,
Universität Erlangen–Nürnberg-Physikalisches Institut, Universität Freiburg-Physikalisches
Institut, Universität Mainz-Institut für Kernphysik,
Technische Universität München, Physik Dept.
INDIA: Matrivani Institute of Experimental Research & Education
ISRAEL: Tel Aviv University, School of Physics and Astronomy
ITALY: University of Eastern Piedmont, University of Trieste-Dept. of Physics, Trieste Section
of INFN, Abdus Salam ICTP, University of Turin-Dept. of Physics, Torino Section of INFN,
JAPAN: Yamagata University, Nagoya University, University of Miyazaki,
POLAND: National Centre for Nuclear Research, University of Warsaw-Faculty of Physics,
Warsaw University of Technology, Institute of Radioelectronics
PORTUGAL: University of Aveiro, Dept. of Physics, LIP
RUSSIA: Joint Institute for Nuclear Research, Lebedev Physical Institute , State Scientific
Center Institute for High Energy Physics of National Research Center 'Kurchatov Institute',
Tomsk Polytechnic University
TAIWAN: Academia Sinica, Institute of Physics
USA: University of Illinois at Urbana-Champaign, Dept. of Physics

LHEP participants (20):
Anosov V.A., Astakhov V.I., Akhunzyanov R.R., Batozckaya V.S., Gavrishchuk O.P., Gushterski R.I, Ivanov A.V., IvanshinY.I., Kisselev Y.F. ,Kouznetsov O. M., Meshcheryakov G.V.,Mitrofanov N.O., Nagaytsev A.P., Peshekhonov D.V., Rogacheva N.S., Salmina E.A., Savin I.A., Smirnov G.I., Yukaev A.I., Zemlyanichkina E.V.

LNP participants (25):
Abazov V.A.,Alexeev G.D., Anfimov N.V., Antoshkin A.I., Chirikov-Zorin I.E., Gridin A.O., Golovanov A. V., Gromov V.O., Guskov A.V., Denisenko I.A., Fedoseev D.V. , Frolov V.N., Jouravlev N.I., Maltsev A.V., Mitrofanov Ye.O., Nikitin M.V., Olchevski A.G. , Piskun A., Rezinko T.V., Rybnikov A.V., Rymbekova A.A.,Samartsev A.G. Selyunin A.S. , Tokmenin V.V., Tchalyshev V.V.

LTP participants (2): Arbuzov A.A., Efremov A.V.

INRNE, Sofia, Bulgaria (1): Gushterski R.I.

Prague Charles University (2): Slunechka M., Janata A.

LEADER	A.P. NAGAYTSEV
DEPUTY	A.V. GUSKOV
SCIENTIFIC LEADER	I.A. SAVIN

PROJECT SUBMISSION DATA IN
SCIENCE ORGANIZATION AND INTERNATIONAL COOPERATION OFFICE 25.04.2017

DATE OF SC LHEP 30.03.2017

DATE OF REPRESENTATION OF PHYSICAL MOTIVATION AT THE LABORATORY SEMINAR: 17.03.2017, 26.10.2016, 03.04.2015

ФОРМА № 25

STUDIES OF THE NUCLEON AND HADRON STRUCTURE AT CERN
COMPASS-II
THEME CODE: 02-0-1085-2009/2019

Project leader: A.P.Nagaytsev

APPROVED BY JINR DIRECTOR	_____	«____»_____20
ENDORSED BY		
JINR VICE-DIRECTOR	_____	«____»_____20
CHIEF SCIENTIFIC SECRETARY	_____	«____»_____20
CHIEF ENGINEER	_____	«____»_____20
HEAD OF SCIENCE ORGANIZATION DEPARTMENT	_____	«____»_____20
LABORATORY DIRECTOR	_____	«____»_____20
LABORATORY CHIEF ENGINEER	_____	«____»_____20
PROJECT LEADER	_____	«____»_____20
PROJECT DEPUTY LEADERS	_____	«____»_____20
ENDORSED		
RESPECTIVE PAC	_____	«____»_____20

ФОРМА № 25

ИЗУЧЕНИЕ СТРУКТУРЫ НУКЛОНОВ И АДРОНОВ В ЦЕРН
COMPASS-II
КОД ТЕМЫ: 02-0-1085-2009/2019

Руководитель проекта: А.П.Нагайцев

УТВЕРЖДЕН ДИРЕКТОРОМ ОИЯИ _____ «____»_____**20**

СОГЛАСОВАНО

ВИЦЕ-ДИРЕКТОР ОИЯИ _____ «____»_____**20**

ГЛАВНЫЙ УЧЕНЫЙ СЕКРЕТАРЬ _____ «____»_____**20**

ГЛАВНЫЙ ИНЖЕНЕР _____ «____»_____**20**

НАЧАЛЬНИК НОО _____ «____»_____**20**

ДИРЕКТОР ЛАБОРАТОРИИ _____ «____»_____**20**

ГЛАВНЫЙ ИНЖЕНЕР ЛАБОРАТОРИИ _____ «____»_____**20**

РУКОВОДИТЕЛЬ ПРОЕКТА _____ «____»_____**20**

ЗАМ. РУКОВОДИТЕЛЯ ПРОЕКТА _____ «____»_____**20**

ОДОБРЕН

ПКК ПО НАПРАВЛЕНИЮ _____ «____»_____**20**

CONTENT

1. INTRODUCTION.

COMPASS is a high-energy physics experiment at the Super Proton Synchrotron (SPS) at CERN in Geneva. The purpose of this experiment is the study of hadron structure and hadron spectroscopy with high intensity muon and hadron beams.

On February 1997 the experiment was approved conditionally by CERN and the final Memorandum of Understanding was signed in September 1998. The spectrometer was installed in 1999 - 2000 and was commissioned during a technical run in 2001. Data taking started in summer 2002 and continued until fall 2004. After one year shutdown in 2005, COMPASS resumed data taking with a muon beam in 2006 and 2007. The years 2008 and 2009 were dedicated to the COMPASS hadron spectroscopy programme with pion and proton beam. In 2010 and 2011 spin structure function measurements with a polarised proton target were performed.

Despite the success of numerous experiments with colliding beams which certainly bring us to the frontier of particle physics, they have not been able to fully replace experiments with a fixed target. The luminosity that can be reached in the beam–target interactions is many orders of magnitude higher than the luminosities reached by colliders. Fixed-target experiments provide a unique possibility to operate with beams of unstable particles, such as muons, pions and kaons. Studying particle interactions with different nuclei is also much simpler with a fixed target. Therefore, fixed-target experiments remain important instruments in particle physics for center-of-mass energies below 50 GeV.

In 2010 an extension of the COMPASS program has been approved by the CERN Research Board. It consists in a set of measurements to study the structure of hadrons in Deep Virtual Compton Scattering (DVCS), Hard Exclusive Meson Production (HEMP), SIDIS, Polarized Drell-Yan and Primakoff reactions [1]. Further investigations in the field of hadron spectroscopy were envisaged as well. On January 2013 a new Memorandum of Understanding was signed, in order to fulfill this program.

In 2012 the data to study the Primakoff reaction were taken. The first (pilot) run for the DVCS measurement was also done. The first-ever polarised Drell-Yan measurement with a beam of negative pions and a polarised proton target was succesfully performed in 2015. Now the experiment has been modified for the 2016/2017 GPD runs with a liquid hydrogen target and a muon beam.

Nearly 220 physicists from 13 countries and 37 institutions work in COMPASS.

JINR team brought a real material and intellectual contributions in COMPASS and COMPASS-II experiments. Our experts participated in development, production and operation of a hadron calorimeter (HCAL1), the muon detector (MW1) and the drift "straw" cameras entering the first spectrometer. Besides, preparation and maintenance of all above mentioned detectors and DAQ system before and during the data taking are traditionally carried out by our experts. The engineering infrastructure of COMPASS is supported by experts from JINR a lot of years. The world's leading specialists in polarized targets from JINR participated in upgrades and maintenance of the target, his work in many respects determines record parameters of a target COMPASS.

In this document we request to prolong the COMPASS project and theme at JINR up to end of 2019. This period covers a continuation of analysis of the data taken up to 2016, preparations of equipment’s and data taking in 2017-2019.

2. COMPASS experiment.

The COMPASS experiment makes use of the CERN SPS high-intensity muon and hadron beams for the investigation of the nucleon spin structure and the spectroscopy of hadrons [2], [3]. The setup is built using several types of tracking detectors, according to the expected incident rate, required space resolution and the solid angle to be covered. Particle identification is achieved using a RICH counter and both hadron and electromagnetic calorimeters.

2.1 Beams

Secondary negative and positive muon and hadron beams, produced by 400 GeV/c protons from the CERN SPS at a primary production target can be extracted to the COMPASS target. Positive muons of 160 GeV/c (2002-2007, 2010) and 200 GeV/c (2011) with an intensity of up to 4×10^7 s^{-1} were used for the COMPASS muon programme. A negative muon beam of 190 GeV/c was used in 2009 and 2012 for pion polarizability measurement as a reference. Positive and negative muon beams of 160 GeV/c will be used for the GPD programme (2016-2017). A negative hadron beam of 190 GeV/c mainly composed of pions, was used for data taking in 2008, 2009 and 2012 hadron runs as well as for the Drell-Yan programme in 2014-2015. Measurements with a positive 190 GeV/c hadron beam, mainly composed of protons, were also performed in 2008. The nominal intensity of the hadron beams was 5×10^6 s^{-1} (up to 8×10^7 s^{-1} for Drell-Yan measurements). The particle composition of the hadron component of the beam is given in Table 1.

Table 1: Relative composition of the hadron beam at the COMPASS target for 190 GeV/c

Particles	Positive beam	Negative beam
π	0.240	0.968
K	0.014	0.024
p	0.746	0.008

It does not include the muon component, which is present on the level of about 1% and negligibly small admixture of electrons and positrons. Two Cherenkov detectors, CEDARs, are installed 30 m before the COMPASS target region. They were designed to provide fast beam particle identification at high rates for particle momenta of up to 300 GeV/c. They are mainly used for kaon/pion separation. The full list of data sets collected (and planned) by COMPASS is presented in Table 2. Large number of different combinations of beams and targets makes COMPASS a unique instrument for the hadron spectroscopy and study of the hadronic interactions.

Table 2: Data sets collected by COMPASS

Year	**Target**	Beam particle	Beam momentum,GeV/c
2002	^{6}LiD	μ+	160
2003	^{6}LiD	μ+	160
2004	^{6}LiD	μ+	160
2006	^{6}LiD	μ+	160
2007	NH_3	μ+	160
2008	Liquid H_2	K- , π-	190
2009	Liquid H2, Ni,W,Pb	μ- , K- , π-	190
2010	NH_3	μ+	160
2011	NH_3	μ+	200
2012	Ni, C,W,Pb	μ- , K- , π-	190
2014	NH_3, W, Al	π-	190
2015	NH_3, W, Al	π-	190
2016	Liquid H_2	μ±	160
2017	Liquid H_2	μ±	160 (planned)
2018	NH_3, W, Al	π-	190 (planned)

2.2 Target zone

The target region for the muon programme is occupied by the cryogenic ^{6}LiD (2002–2006) and NH_3 (2007–2011) targets subdivided into two (2002–2004) and three (2006–2011) cylindrical cells placed along the beam direction. The target material of each individual cell was longitudinally or transversely polarized. A liquid hydrogen target was mainly used for data taking with hadron beam in 2008 and 2009. The target is surrounded by a time-of-flight Recoil Proton Detector (RPD). Precise silicon tracking detectors are installed up- and downstream of the target. In 2009 and 2012 the liquid hydrogen target was removed and replaced with a specially designed solid-target holder where up to 16 solid targets with different atomic numbers and different thicknesses were mounted. Nickel, carbon, tungsten and lead targets were used (see Table 2). A two-cell polarized ammonia target (55 mm + 55 mm) was used in 2014 and 2015 for the Drell-Yan data taking with a negative pion beam [4]. In order to reduce occupancy of downstream detectors a thick hadron absorber made of aluminium, alumina (Al_2O_3) and stainless steel was placed immediately downstream the polarized target. The inner part of the absorber contains a tungsten beam plug which can also be treated as an additional target. A small aluminium target was also installed in front of the beam plug.

For the data taking within the framework of the GPD programme, in 2016 and 2017 a 2.5-meter long liquid hydrogen target will be used [5].

2.3 Spectrometer

The COMPASS spectrometer is designed to reconstruct scattered muons and produced hadrons in wide momentum and angular ranges. It consists of two stages, each equipped with a dipole magnet, to measure tracks with large and small momenta, respectively. In the high-flux region, in or close to the beam, tracking is provided by stations of scintillating fibres, silicon detectors, micromesh gaseous chambers and gas electron multiplier chambers. Large-angle tracking devices are multiwire proportional chambers, drift chambers and straw detectors. Muons are identified in large-area mini drift tubes and drift tubes placed downstream of hadron absorbers. Each stage of the spectrometer contains an electromagnetic and a hadron calorimeter. The identification of charged particles is possible with a RICH detector, although in this analysis it is not used. A detailed description of the experiment can be found in [2,3].

The COMPASS setup can be divided into four parts along the beam, starting with the beam line sectionand the detectors that identify the incoming beam particles. It is followed by the target region, which is specific for each of the COMPASS physics programmes. It comprises the target and the detectors located in its near vicinity. The third part, called Large Angle Spectrometer (LAS) includes the first dipole magnet, SM1, the tracking detectors around it, and the RICH-1 counter. The fourth part, called Small Angle Spectrometer (SAS), occupies the downstream part of the setup. It is built around the SM2 dipole magnet and includes several tracking detectors. Both LAS and SAS comprise a pair of electromagnetic and hadron calorimeters, and a muon filter. Figure 1 shows the three-dimensional and top views of the COMPASS setup.

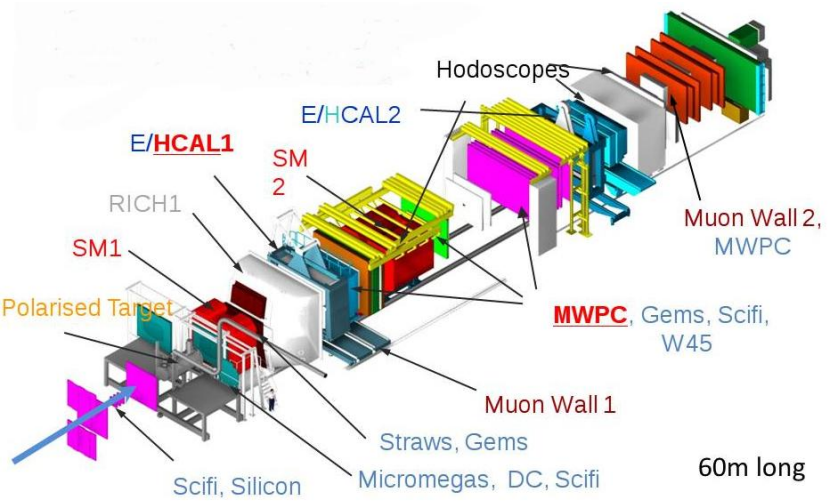

Figure 1: 3D view of the COMPASS setup (2002-20011 data taking).

One of the main objectives of the COMPASS-II is the study of functions of generalized parton distributions (GPD) in nucleons. The GPD concept has attracted great attention of scientists after it was shown that the total angular momentum of a certain type of partons, J^f for quarks ($f = u; d$ or s) or J^g for gluons, which depends on the second moment of the sum of two GPDs H and E. Collecting data for these GPDs via measurement of exclusive Deep Virtual Compton Scattering (DVCS), $\mu\ p \rightarrow \mu\gamma p$, or High Energy Meson Production (HEMP), $\mu\ p \rightarrow \mu M p$, is the only known method to determine the components of the "contribution" to the nucleon spin $1/2 = \sum_{f=u;d;s} (J^f + J^g)$. The DVCS and HEMP reactions are exclusive. In order to measure their cross-sections, the existing setup COMPASS should be upgrated by 2 new detectors – Proton Recoil Detector (the RPD), which measures characteristics of protons, and the electromagnetic calorimeter ECAL0 in front of the first spectrometer magnet (SM1) (Figure.2).

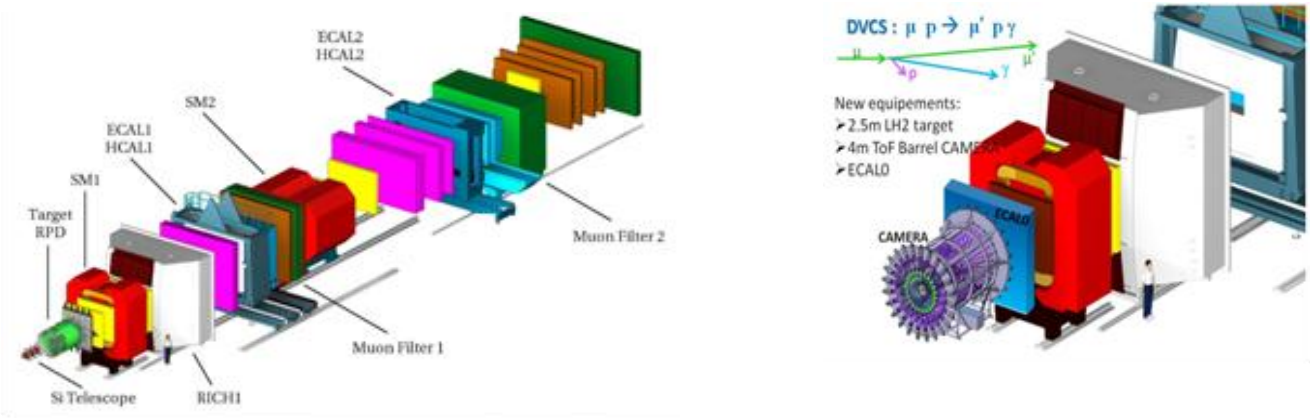

Figure 2: Experimental COMPASS setup (left) and the front of the spectrometer, upgrated by the detectors for studying of generalized parton distributions.

For the second part of COMPASS programme - Drell-Yan measurement, a negative pion beam of 190 GeV/c momentum is used. The target consists of 2 target cells, with 55 cm length and 2 cm radius each, and spaced by 20 cm. As used in the past COMPASS SIDIS measurements, the target material is a solid state ammonia (NH_3). Using a dipole field to keep the proton spins in the target transversely polarized with respect to the pion beam direction, one can reach up to 90% polarization, with a dilution factor (which refers to the fraction of polarizable material in the target) of 20%. The 2 target cells are oppositely polarized, and spin reversal is performed every few days, in order to minimize some of the systematic errors in the azimuthal spin asymmetries extraction. In order to have meaningful statistics, the relatively low cross-section of the Drell-Yan process must be compensated by a high intensity pion beam. The maximum beam intensity achievable in COMPASS is used, 108 particles per second, the limit being dictated by the beam line itself, the allowed radiation dose in the hall, and to avoid local heating of the target (that could compromise the target

polarization). In order to keep the detectors occupancy at reasonable level below 5%, a thick hadron absorber is placed immediately downstream the polarized target (see Figure 3).

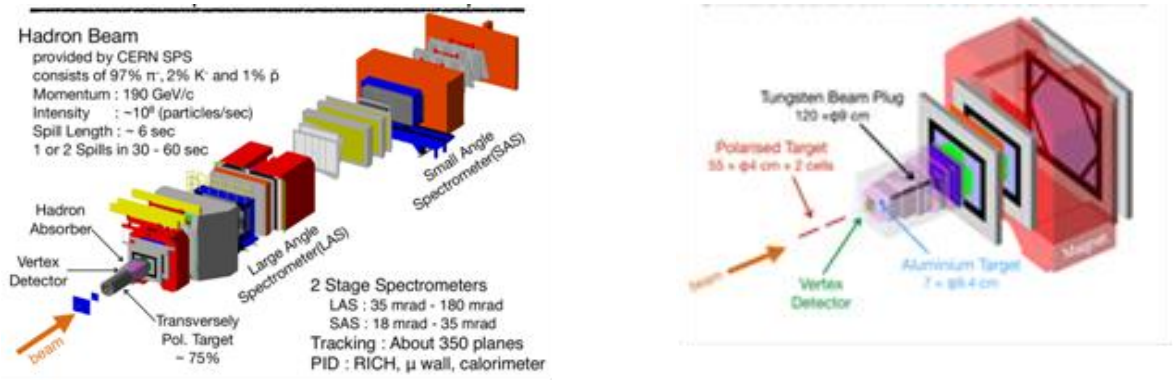

Figure 3: The COMPASS spectrometer for DY measurements (left panel). The target region with hadron absorber (right panel).

The obligations of the JINR concern the HCAL1, MW1, and new electromagnetic calorimeter ECAL0

2.4 Muon wall 1

The basic element of the MW1 system is the gaseous wire detector called Mini Drift Tube (MDT). The geometry is based on plastic streamer tubes (see reviews in [6,7]). A modified version of the MDTs with fully metallic cathodes was produced for the COMPASS experiment. The MDT is working in proportional mode. This allows the detector to withstand the high-rate background conditions of the COMPASS experiment. An MDT module consists of an eight cell aluminium comb extrusion with a wall thickness of 0.6 mm covered on top by a 0.15 mm thick stainless steel foil, gold plated tungsten wires (50 μm in diameter) strung in the centre of the cells and an ABS plastic envelope (sleeve) with thickness around 1 mm to house the interior of the module. The wires are thermally glued to polyethylene plastic spacers (not shown on Fig. 4) at equal distances of less than 1 m along the length of the MDT to provide electrostatic stability. The wire pitch is 10 mm. The two end plugs are thermally welded at the ends of the MDT, thus forming together with the envelope the gas-tight volume of the module. The plastic envelope also serves for the HV insulation as the negative voltage is applied to the metallic cathode. The anode wires are grounded through the input of amplifiers. Details of the manufacturing and the testing are given in [8,9]. The schematic view of the MW1 system is shown in Fig. 4. The system consists of two stations separated by a 60 cm thick iron absorber. Each station has four detectors with two planes of MDTs on both sides. Vertical and horizontal tubes provide the X and Y coordinates, respectively. The outer surface of each station is covered with thin (1 mm thick) aluminium sheets for mechanical, electrostatic and noise protection.

The whole MW1 system showed very stable performance during nominal data taking conditions.

The value of the obtained efficiency is typically 91%, close to the geometrical one for the MDT detectors plane of 88.5% (just few percent higher due to the small divergence of the halo muons). The variation of the single plane efficiencies of about 1% diminishes to 0.2% when using the whole MW1 system with at least five (out of eight) points for a track.

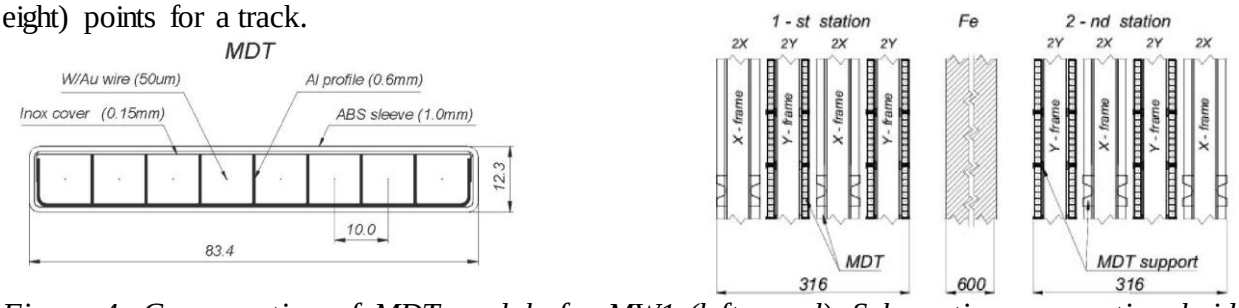

Figure 4: Cross section of MDT module for MW1 (left panel). Schematic cross-sectional side view of MW1 (right panel).

2.5 HCAL1

The hadron calorimeter 1 (HCAL1) is placed (see Fig. 1) before MW1. HCAL1 has a modular structure, each module consisting of 40 layers of iron and scintillator plates, 20 mm and 5 mm thick, respectively, amounting to 4.8 nuclear interaction lengths. The structure of a calorimeter module and its basic dimensions are shown in Fig. 5 [10].

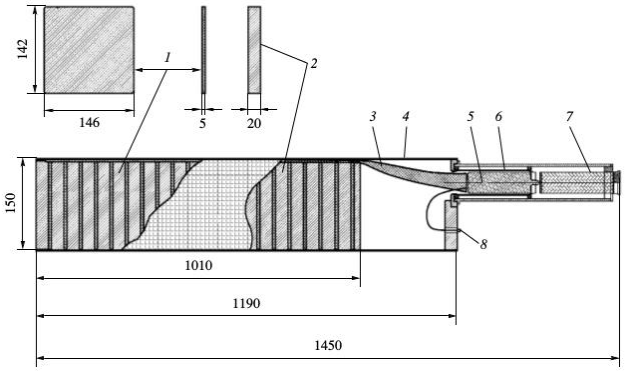

Figure 5: Structure of the HCAL1 module: 1-scintillators, 2-iron plates, 3-light guide, 4-container, 5-PMT, 6-PMT magnetic shielding, 7-Cockcroft-Walton divider, 8-optical connector for LED control. Dimensions are in mm.

Monte Carlo simulations for hadrons and electrons were performed in the 10 – 100 GeV energy range. These particles are almost fully absorbed in such a calorimeter. The 480 calorimeter modules were assembled and framed in a matrix of 28 (horizontal) × 20 (vertical) with 12 modules removed from each corner. There is a rectangular window of 8 × 4 modules at the centre of the matrix for the passage of the beam and scattered muons. The outside dimensions of the HCAL1 are 4.2 × 3 m^2 and useful surface is 10.8m^2. The calorimeter and its frame are mounted on a platform which can be moved across the beam axis. The resolution of a sampling calorimeter depends on the qualities of scintillators, light guides and PMTs. The scintillators of HCAL1 have been produced by molding under pressure from granulated polystyrene PSM-115 mixed with P-terphenyl (1.5%) and POPOP (1,4-Bis-[2-(5- Phenyloxazolyl)]-Benzene) (0.04 %). The light from the scintillators is collected by a single flat light guide placed on the open sides of the scintillators with an air gap of 0.6 – 0.8 mm. The wavelength shifting light guides are fabricated from organic glass (CO-95, CO-120) and painted by cumarine K-30 solved in alcohol. The amount of light emitted and collected from a single scintillator traversed by a minimum ionising particle is enough to produce 4– 6 photoelectrons at the PMT photocathode (12-cascade FEU-84-3 PMT). They have multi-sodium photocathodes with quantum efficiencies between 0.18 and 0.26 at the wavelength of 460 nm, a large dynamic range, currents up to 5 mA, a typical pulse rise time of 15 – 18 ns and a full pulse width of 40 – 50 ns at the level of 0.1 of its amplitude. A Cockcroft-Walton voltage multiplication scheme is used to supply the PMT dynodes with high voltages from the basic 100 V. The signals from the PMTs are sent via 50 Ω cables of about 140 m length to fast analogue-to-digital converters (see Sec. 8.3.2). Small fractions of the signals are fed into the fast summation system for trigger purposes (see Sec. 7.1.2). The main characteristics of the calorimeter – linearity of the response versus energy, e/π ratio, energy and space resolutions – were determined using the negative hadron and lepton beams at the CERN X5 beam line with energies between 10 and 100 GeV. The energy resolution of HCAL1 as a function of the energy for pions √ can be parameterized by $\sigma(E)/E = (59.4 \pm 2.9)\ \%/\sqrt{E} \oplus (7.6 \pm 0.4)\ \%$, with the energy E in units of GeV. A similar dependence is expected from MC simulations. The average value of the e/π ratio, calculated from the positions of the electron and pion ADC spectra at the same energy, is 1.2 ± 0.1. The spatial resolution $\sigma_{x,y}$ = 14 ± 2 mm was measured by scanning the beam over the central module of a 5 × 5 matrix and determining of the shower centre of gravity.

2.6 ECAL0

The new calorimeter of ECAL0 provides registration of events in significantly wider kinematic region of response in comparison with the existing calorimeters of ECAL1 and ECAL2. ECAL0 was proposed and developed at JINR in collaboration with groups of physicists from Munich, Freiburg, Warsaw, Saclay (France), Prague, CERN and colleagues from Kharkov (Ukraine). The new electromagnetic calorimeter is a unique device, "shashlyk"-type (scintillator, lead), in which the most advanced photodetectors – Micro-pixel Avalanche Photo Diodes (MAPD) with ultra-high pixel density (up to 15 thousand pixels / mm^2) were applied, instead of the traditional photomultiplier tubes. So, it was the first time when the MAPD were applied for the electromagnetic calorimeter at large physical setup. It should be noted that for more than 20 years this type of photo detector has been developed and tested in many institutions, and JINR is one of the leading centers in this field. The MAPD with the pixel density (15 thousand pixels / mm^2) were developed in our institute and were used in the calorimeter as a part of the experimental setup COMPASS in 2012 during the pilot data taking. To serve this purpose, more than a quarter of the calorimeter modules were produced. After successful tests the final stage of production of a calorimeter was begun and 250 modules were produced and tested at Institute of Scintillation Materials (ISMA, Kharkiv, Ukraine). In December 2013 the modules were delivered to CERN. Further tests of the MAPD calorimeter were associated with new physical tasks – the use of this detector in intense hadron beams – led to the need to use a new fast MAPD of MPPC S12572-10P-type of Hamamatsu company (10 thousand pixels/mm^2). Development, production and testing of the registration blocks on the basis of these MAPD took almost one and a half year and were successfully completed in cooperation with the Russian company Rusalox (Vladimir). This Russian company is a manufacturer of motherboards with high thermal conductivity of the aluminaoxid-based technology that provides high cooling efficiency of any heat-electronic components. Printed circuit boards manufactured with this technology are made of a conducting layer of aluminum and a dielectric material with nanopourous structure. We needed a new technological process - drilling holes, their oxidation and metallization, with leakage currents on the level of a pA at the voltage of 100 V. Additionally JINR performed soldering of the pins and gluing the MAPD to the alumina board, gluing Winston cones to the MAPD and other operations of assembly of the registering units were performed. The first recording blocks were ready in the beginning of June 2015 and at the end of June 2015 20 recording blocks were delivered to CERN and tested on the beam. As a result - after many years of hard work on the development and optimization of the detector systems, many unit prototype tests and calorimeter reading system beams tests at CERN, at DESY (Hamburg) and at complex ELSA (Bonn) the final version of the module calorimeter was developed which is shown in Figure 6.

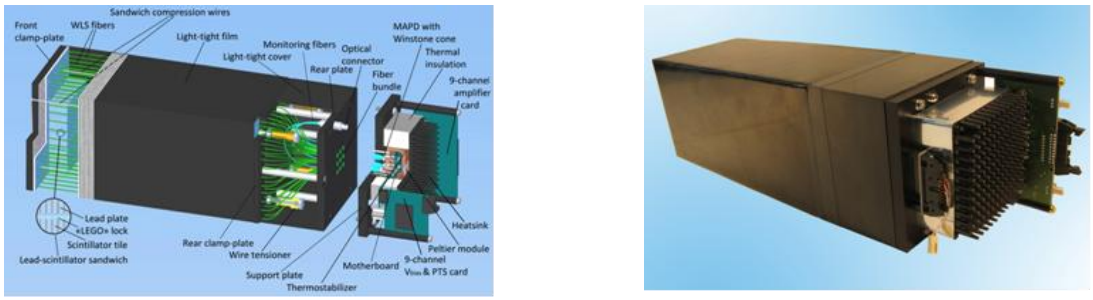

Figure 6:ECAL0 calorimeter module.

It is important to mark that groups of other scientific centers and production companies took part in development of systems of a calorimeter. Except the colleagues who are already mentioned above from ISMA and Rusalox, power system, monitoring and thermostabilizaton systems were developed and produced by HVSYS firm, system of reading (ADC) and amplifiers were created by groups from Munich and Warsaw, and the group from Prague produced optical splitters for system of ECAL0 slow control and monitoring.

In March-April 2016 the ECAL0 was fully assembled, tested and included in the COMPASS setup, and currently is successfully used for data taking. The main features of the new calorimeter can be formulated as follows: ECAL0 effectively registers direct photons of the DVSC and DVMP reactions in a wide energy range

(0.2 - 40GeV); and together with ECAL1 (Fig. 2) effectively registers π^0, which can significantly reduce the background of photons, which are produced by π^0; provide an opportunity for additional measuring reactions with the release of other mesons. These properties significantly expand our measuring range with minimal systematic uncertainties.

The ECAL0 consists of: 194-tower modules, 1746 MAPDs and readout channels; 28 MSADCs and HV system with temperature stabilization, power suppliers and slow control.

Stable operation of our calorimeter within the first months of a data taking was appreciated by the leaders of the COMPASS collaboration (see Fig.8). We expect to obtain new physical results with data from the ECAL0 already in 2017. Besides, the obtained experience will be used by development of similar calorimeters for MPD and SPD setups in the NICA complex.

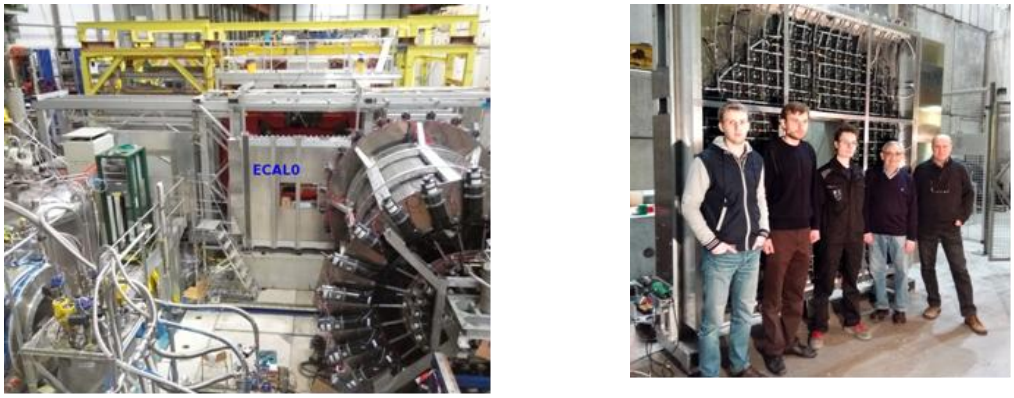

Figure 7: Assembled and ready to work calorimeter as a part of the COMPASS setup(left). JINR team participated in ECAL0 assembling (right).

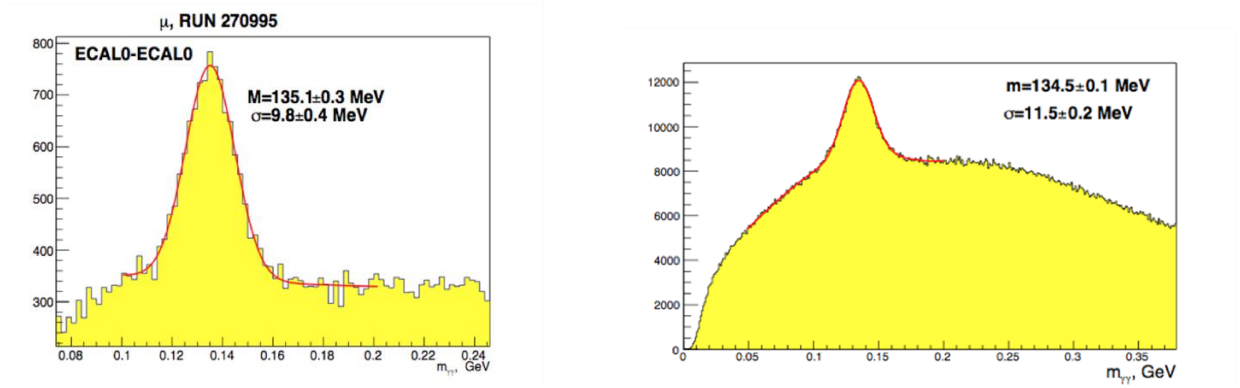

Figure 8: Typical γγ spectra from ECAL0 (2016 data taking) with muon(left panel) and pion (right panel) beams.

2.4 Participation in data taking

The data taking is planned to be executed in 2017 and 2018. Every year duration of a data taking is about 7 months. Every day the data taking is divided into 3 shifts, on 2 physics in each shift. According to safety rules for CERN, presence of participants of shifts in the Control room of COMPASS is obligatory. It is explained by existence in the setup of a liquid hydrogen target, RICH detector and some other systems which demand permanent operating control. The number of shifts per year for each group is defined by number of authors and PhD students. The JINR fraction of authors and PhD students is about 1/6 from all authors and PhD students of collaboration. Thus, total number of shifts for our group in a year - about 200.

In 2017 COMPASS will take data on the program of GPD measurements. According MoU, the JINR group is obliged to support 3 detectors: hadron calorimeter HCAL1, coordinate system MW1 and new

electromagnetic calorimeter ECAL0. One needs presence of oncall experts for all time of a data taking. Constantly 2 oncall experts from our group participate in data taking, one - for MW1, the second – for HCAL1 and ECAL0. These experts also take the shifts, usually – about half of total number of shifts for our group per year. Rest part of shifts covers by JINR group members which are involved in the data analysis, combining work in shifts with reports at various meetings of collaboration and other activities.

In 2018 COMPASS will collect data on the Drell-Yan program. For these measurements only two from three above mentioned detectors will be used – HCAL1 and MW1. The number of authors from the JINR group will be reduced, the smaller number of shifts is expected.

3. MAIN COMPASS –II RESULTS.

Up to now the COMPASS Collaboration has published and submitted 53 papers (see a list in Appendix), 23 of them in 2014-2016. For this period COMPASS members have presented about 250 talks at the International Conferences and workshops.

The recent main COMPASS results published in 2014-2016 are described in this Section.

3.1 Pion polarizability from 2009 data.

In classical physics the dipole electric and magnetic polarizabilites of a medium or a composite system are well-known characteristics related to the response of the system to the presence of an external electromagnetic field. This concept can be extended up to the case of composite particles as hadrons. The electric polarizability α and the magnetic polarizability β describe the rigidity of such objects against the deformation by the external electric and magnetic fields and can be tested in the reaction of Compton scattering off hadron. They are fundamental characteristics of hadron and the comparison of the theoretically predicted and directly measured values provides a stringent test of various theoretical models in the low-energy region.

The Chiral Perturbation Theory (ChPT), the most successful model in the low-energy region, where pion plays role of the Godstone boson, predicts for the charged pion in the two-loop approximation the values $\alpha_\pi - \beta_\pi = (5.7 \pm 1.0)\times 10^{-4}$ fm^3 and $\alpha_\pi + \beta_\pi = 0.16\times 10^{-4}$ fm^3 [11]. The most of other models like linear σ-model with quarks, chiral quark model, super-conductor quark model, quark confinement model, dispersion relations, lattice QCD predict the value of the electric polarizability α_π within the range 3.5×10^{-4} $fm^3 < \alpha_\pi < 7.0\times 10^{-4} fm^3$, larger than ChPT predicts.

Several attempts to measure the pion electric (α_π) and magnetic (β_π) polarizabilities in the dedicated experiments have been performed. The groundbreaking work at Serpukhov used the Primakoff-like process of pion radiative scattering off the nuclear target

$$\pi^-(A, Z) \rightarrow \pi^-(A, Z)\gamma. \quad (1)$$

Pion photoproduction $\gamma p \rightarrow n\pi^+$ was used to determine the pion polarizabilities at Lebedev Institute and MAMI . Certain results were also obtained using the reaction $\gamma\gamma \rightarrow \pi^+\pi^-$ in e^+e_- collisions . The experimental values for the quantity $\alpha_\pi - \beta_\pi$ assuming $\alpha_\pi + \beta_\pi = 0$ are shown in Fig.9(right). These obtained results were affected by large statistical and systematic uncertainties and their accuracy was a few times lower than the precision of theoretical predictions.

The reaction (1) is used to measure the pion polarizabilities at COMPASS. It can be treated as Compton scattering of a virtual photon, provided by a target nucleus, off the pion. The 4-momentum transferred to the nucleus in the reaction is very small ($Q \ll m_\pi / c$). In the center-of-mass system the differential cross section can be described by the formula:

$$\frac{d^3\sigma_{\pi(A,Z)}}{ds dQ^2 d\Omega} = \frac{\alpha Z^2}{\pi(s - m_\pi^2)} \frac{Q^2 - Q^2_{min}}{Q^4} F^2(Q^2) \times \frac{d\sigma_{\pi\gamma}}{d\Omega} \quad (2)$$

where m_π is the pion mass, α is the fine structure constant, s is the squared total energy of the πγ system, $Q^2_{min} = (s - m^2_\pi)^2/4E^2_0$, $F(Q^2) \approx 1$ is the electromagnetic form factor of the nucleus, $d\Phi$ is a phase-spaceelement of the final-state and

$$\frac{d\sigma_{\pi\gamma}}{d\Omega} = \left(\frac{d\sigma_{\pi\gamma}}{d\Omega}\right)_0 - \frac{\alpha\, m_\pi^3 (s-m_\pi^2)^2}{4s^2\,(s\,z_+ + m_\pi^2\, z_-)} \left(z_-^2\,(\alpha_\pi - \beta_\pi) + \frac{s^2}{m_\pi^4} z_+^2 (\alpha_\pi + \beta_\pi) \right) \tag{3}$$

Here $z_\pm = 1 \pm \cos\theta$, where θ is the $\pi\gamma$ scattering angle. Thus the cross section depends on $\alpha_\pi+\beta_\pi$ at forward angles and on $\alpha_\pi-\beta_\pi$ at backward angles. Consequently, pion polarizabilities α_π and β_π can be accessed via precise measurement of energy and angular distributions of produced photons and their comparison with the expectations for the point-like pion.

In 2015 COMPASS published the first result for the pion polarizabilities [12]. It was obtained using the data collected in 2009 with a negative pion beam of 190 GeV/c and a nickel target. The number of collected $\pi\gamma$ events with a photon energy above 76 GeV is 63000. A comparable data sample with a negative muon beam of the same momentum was also collected. Since the muon is a point-like particle, the measured differential cross section should exactly correspond the QED calculations. This muon sample was used to control the possible systematic effects. The ratios R_π and R_μ of the measured differential cross sections over the expected cross sections for the point-like pion and muon as a function of the energy of emitted photon normalized to the beam energy x_γ are shown in Fig. 9 (left). The resulting value $\alpha_\pi = (2.0 \pm 0.6_{stat} \pm 0.7_{syst}) \times 10^{-4}\ fm^3$ was determined assuming $\alpha_\pi+\beta_\pi=0$ from the fit of the function

$$f(x_\gamma) = 1 - \frac{3}{2}\frac{m_\pi^3}{\alpha}\frac{x_\gamma^2}{1-x_\gamma}\alpha_\pi \tag{4}$$

to R_π . The measured ratio R_μ is consistent with the hypothesis of the point-like structureless muon. The obtained result for the pion polarizability is at significant variance with the previous experiments and compatible with the expectation from ChPT. The COMPASS measurement is the most precise dedicated measurement of this value at the moment (see Fig.9 (right)). This result is included as the first entree to the PDG issue of 2016 [13].

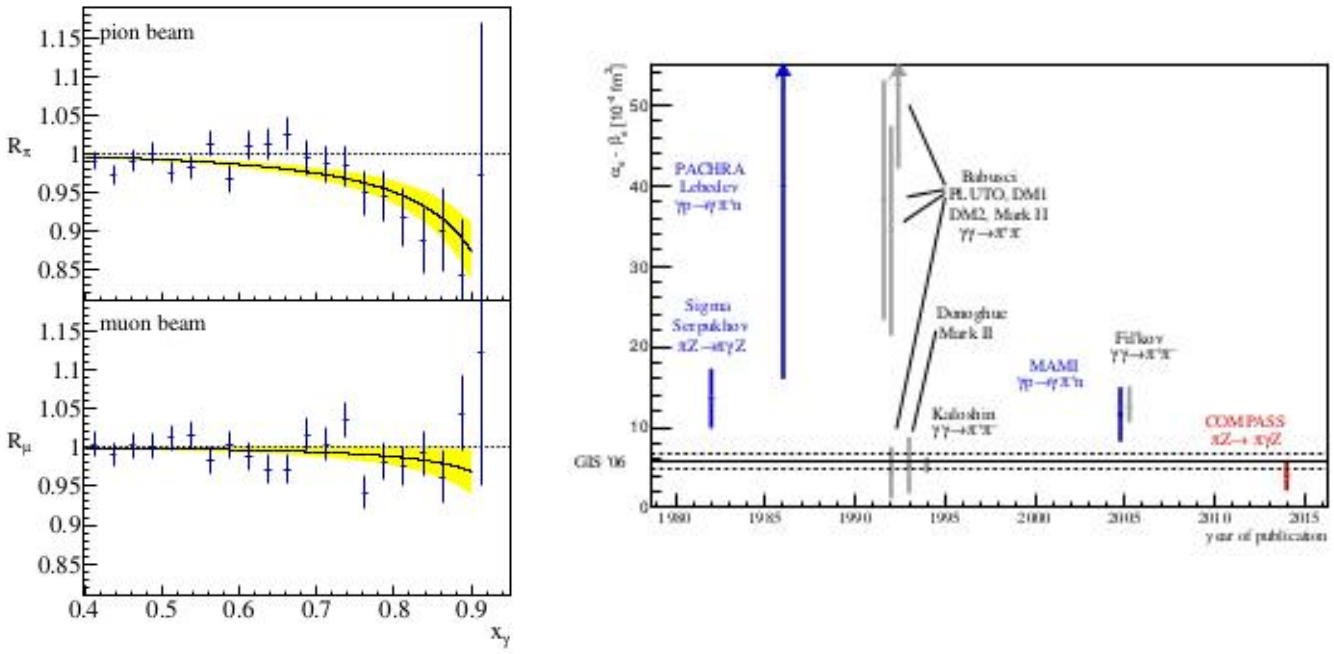

Figure 9: Ratios R_π and R_μ of the measured differential cross sections over the expected cross sections for the point-like pion and muon as functions x_γ (left). Experimental results for the quantity $\alpha_\pi-\beta_\pi$ assuming $\alpha_\pi+\beta_\pi=0$. Horizontal lines represent the prediction of ChPT (right).

3.2 Exclusive photo-(lepto-)production of exotic charmonium $Z_c^\pm$ (3900)

According to QCD quarks and gluons are confined within hadrons. Before the beginning of 2000s only two classes of hadrons were known: mesons (composed of a pair of quark and antiquark) and baryons (composed of

three quarks). Although other states like tetra- and pentaquarks, glueballs and quark-gluon hybrids etc. are not forbidden.

To date, dozens of charmoniumlike states, the so-called XYZ states, have been observed in numerous reaction channels and final states, such as e^+e^- collisions by CLEO-c, BaBar, Belle, BESIII and in hadronic interactions by CDF, D0, LHCb, CMS, and ATLAS. Several interpretations of the new states do exist: pure quarkonia, tetraquarks, hadronic molecules, hybrid mesons with a gluon content, etc. But at the moment many basic parameters of XYZ states have not been determined yet. New experimental input is required to distinguish between the models that provide different interpretations of the nature of these states.

Study of leptoproduction of exotic charmonia is important for clarification of the nature of such states. At the same time it tests the power of the method, which will allow studying exotic charmonium-like states at facilities with intensive photon beams such as CLAS or GlueX.

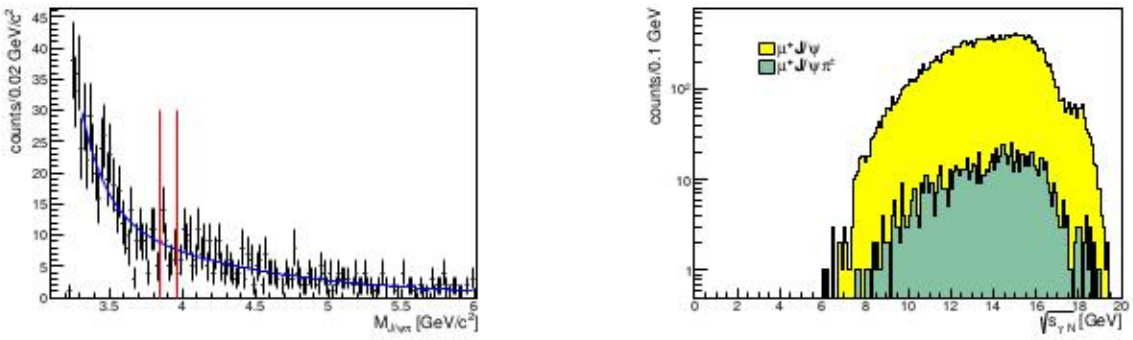

Figure 10: Mass spectrum of the $J/\psi_{\pi\pm}$ state [14] (left). $\sqrt{s}_{\gamma N}$ distribution for exclusive $\mu^+ J/\psi$ and $\mu^+ J/\psi_{\pi\pm}$ events [15] (right)

The COMPASS setup and the COMPASS kinematics are suitable for study of exclusive photo-(lepto-)production of charmonia. On the one hand, the beam energy is high enough to produce a number of interesting final states, on the other hand relatively low multiplicity of secondary particles in combination with the perfect detector provide strict control of exclusivity.

Exclusive leptoproduction of the hadron $Z_c^{\pm}(3900)$, which is the most probable candidate to be a tetraquark, has been searched for at COMPASS in the reaction

$$\mu^+ N \to \mu^+ Z_c^{\pm}(3900) N' \to \mu^+ J/\psi \pi^{\pm} N' \to \mu^+ \mu^+ \mu^- \pi^{\pm} N' \tag{5}$$

using the full set of muon data collected in 2002-2011 [14]. According to the vector meson dominance (VMD) model, a photon may behave like a *J/ψ* so that a $Z_c^{\pm}$ (3900) can be produced by the interaction of the incoming virtual photon, emitted **d** by the incoming muon with a virtual charged pion provided by the target nucleon.

The mass spectrum for $J/\psi_{\pi\pm}$ events is shown in Fig.10 (left). It does not exhibit any statistically significant signal around the nominal mass of $Z_c^{\pm}$ (3900) . The upper limit of the Z_c (3900) production rate was established to be

$$BR(Z_c^{\pm}(3900) \to J/\psi\pi^{\pm}) \times \sigma_{\gamma N \to Z_c^{\pm}(3900)\ N}\Big|_{\langle\sqrt{s_{\gamma N}}\rangle = 13.8\ GeV} < 52\ \text{pb},\ (CL = 90\%). \tag{6}$$

The obtained result was treated within the framework of the production model described in [13]. For the cut-off parameter $\Lambda = 0.6\ GeV$ of the model the upper limit of partial width of the decay $Z_c^{\pm} \to J/\psi_{\pi\pm}$ was estimated to be 2.4 MeV (CL=90%).

The result [15] is included to the PDG review [13].

3.3 Drell-Yan measurements in 2014-2015

The polarized Drell-Yan process (Fig.11) gives an alternative access to TMD PDFs, with the advantage over SIDIS that no fragmentation functions are involved, the measured spin asymmetries relating to convolutions of 2 TMD PDFs.

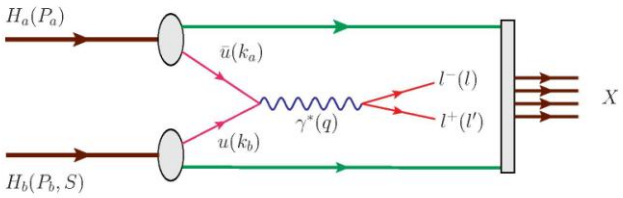

Figure 11: The diagram of the Drell-Yan process.

In leading order QCD, when having a transversely polarized target, the Drell-Yan cross-section can be written in a form that highlights these azimuthal asymmetries, see Equation and Figure with explanation below.

$$\frac{d\sigma}{d^4q d\Omega} = \frac{\alpha^2}{Fq^2}\hat{\sigma}_U \Big\{ (1 + D_{[\sin^2\theta]} A_{UU}^{\cos 2\phi} \cos 2\phi) + |\vec{S}_T| \Big(A_{UT}^{\sin\phi_S} \sin\phi_S + D_{[\sin^2\theta]} \Big(A_{UT}^{\sin(2\phi+\phi_S)} \sin(2\phi+\phi_S) + A_{UT}^{\sin(2\phi-\phi_S)} \sin(2\phi-\phi_S) \Big) \Big) \Big\} \quad (7)$$

The 4 azimuthal asymmetries give access to the following convolutions:
- the Boer-Mulder TMD from pion with Boer-Mulders from proton for $A_{UU}^{cos2\varphi}$;
- the unpolarized TMD from pion with Sivers TMD from proton for $A_{UT}^{sin\varphi S}$;
- the Boer-Mulders TMD from pion with pretzelosity TMD from proton for $A_{UT}^{sin(2\varphi+\varphi S)}$;
- the Boer-Mulders TMD from pion with transversity TMD from proton for $A_{UT}^{sin(2\varphi-\varphi S)}$.

$$\begin{aligned} &d\sigma(\pi^- p^\uparrow \to \mu^+\mu^- X) = \\ &= 1 + \overline{h}_1^\perp \otimes h_1^\perp \cos(2\phi) \\ &+ |S_T| \; \overline{f}_1 \otimes \overline{f}_{1T}^\perp \sin\phi_S \\ &+ |S_T| \; \overline{h}_1^\perp \otimes h_{1T}^\perp \sin(2\phi + \phi_S) \\ &+ |S_T| \; \overline{h}_1^\perp \otimes h_1 \sin(2\phi - \phi_S) \end{aligned}$$

beam pion — target proton

Figure 12: The cross section of the Drell-Yan process via PDFs.

Due to their naive time reversal odd nature, Sivers and Boer-Mulders TMD PDFs change sign when accessed from DY or from SIDIS. The experimental observation of this sign-change is considered a crucial test of the TMD approach of non-perturbative QCD.

The Drell-Yan data taking has started in 2014 with pilot run. Preliminary about 7K DY events and about 200 K J/Ψ events were collected during three weeks of stable data taking. In 2015 COMPASS has taken about 35K DY events in 4.5 months of stable data taking. The di-muon spectra obtained in 2015 data is shown in Fig.13.

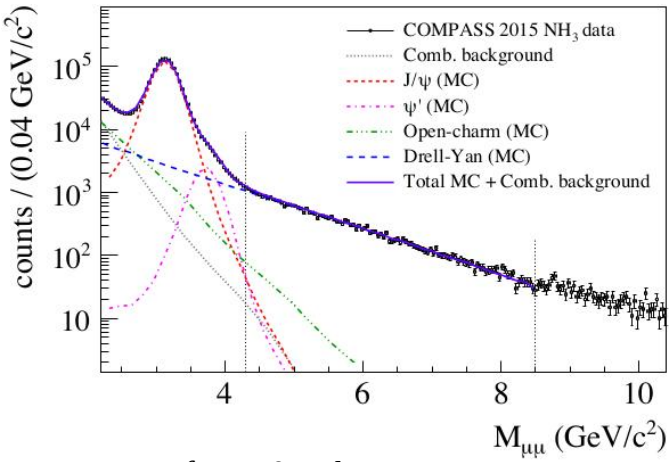

Figure 13: The di-muon spectra from 2015 data.

The analysis of the collected data are in progress.

3.4 DIS and SIDIS results

New results for the double spin asymmetry A_1^p and the proton longitudinal spin structure function g_1^p were obtained by the COMPASS collaboration using polarised 200 *GeV* muons scattered off a longitudinally polarised NH_3 target [16] (Fig.14). The data were collected in 2011 and complement those recorded in 2007 at 160 *GeV*, in particular at lower values of x. They improve the statistical precision of $g_1^p(x)$ by about a factor of two in the region $x \sim 0.02$.

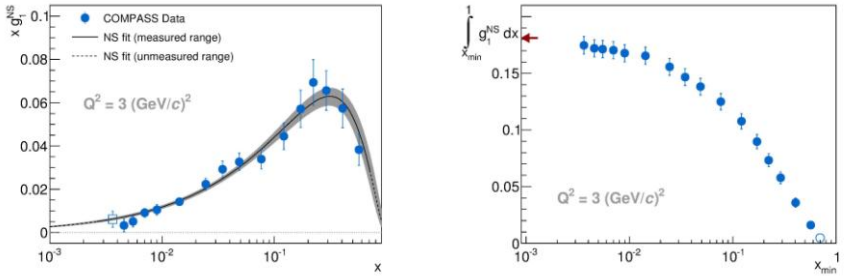

Figure 14. Left panel:The asymmetry A_1 as a function of x at the measured values of Q^2 as obtained from the COMPASS data at 200 GeV. Right panel: The spin-dependent structure function xg_1 at the measured values of Q^2 as a function of x.

A next-to-leading order QCD fit to the g_1^p world data is performed. It leads to a new determination of the quark spin contribution to the nucleon spin, $\Delta\Sigma$ ranging from 0.26 to 0.36, and to a re-evaluation of the first moment of g_1^p.

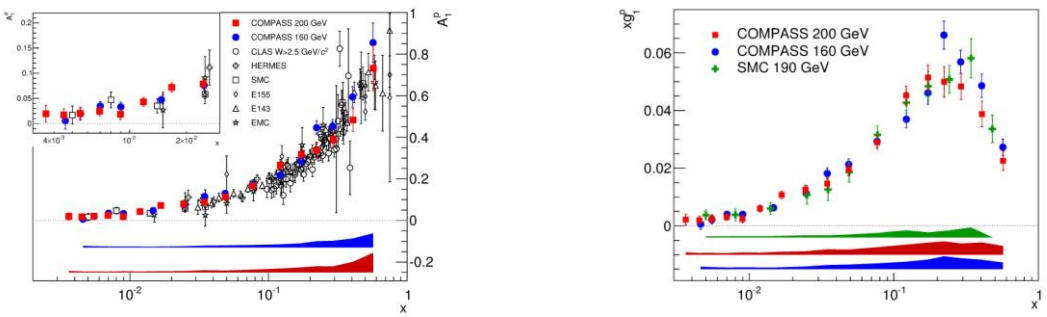

Figure 15: Left panel: Values of $xg_1^{NS}(x)$ at Q^2 = 3 $(GeV/c)^2$ compared to the non-singlet NLO QCD fit using COMPASS data only. Right panel:Values of integral of g_1^{NS} over x for region between x_{min} and 1 as a function of x_{min} .

The uncertainty of $\Delta\Sigma$ is mostly due to the large uncertainty in the present determinations of the gluon helicity distribution. A new evaluation of the Bjorken sum rule based on the COMPASS results for the non-singlet structure function $g_1^{NS}(x,Q^2)$ yields as ratio of the axial and vector coupling constants $|g_A/g_V| = 1.22 \pm 0.05$ (stat.) $\pm$ 0.10 (syst.), which validates the sum rule to an accuracy of about 9% (Fig.15).

Single hadron azimuthal asymmetries in the cross sections of positive and negative hadron production in muon semi-inclusive deep inelastic scattering off longitudinally polarised deuterons are determined using the 2006 COMPASS data and also all deuteron COMPASS data. For each hadron charge, the dependence of the azimuthal asymmetry on the hadron azimuthal angle φ is obtained by means of a five-parameter fitting function that besides a φ-independent term includes four modulations predicted by theory: $sin\varphi$, $sin2\varphi$, $sin3\varphi$ and $cos\varphi$ [17] (Fig.16).

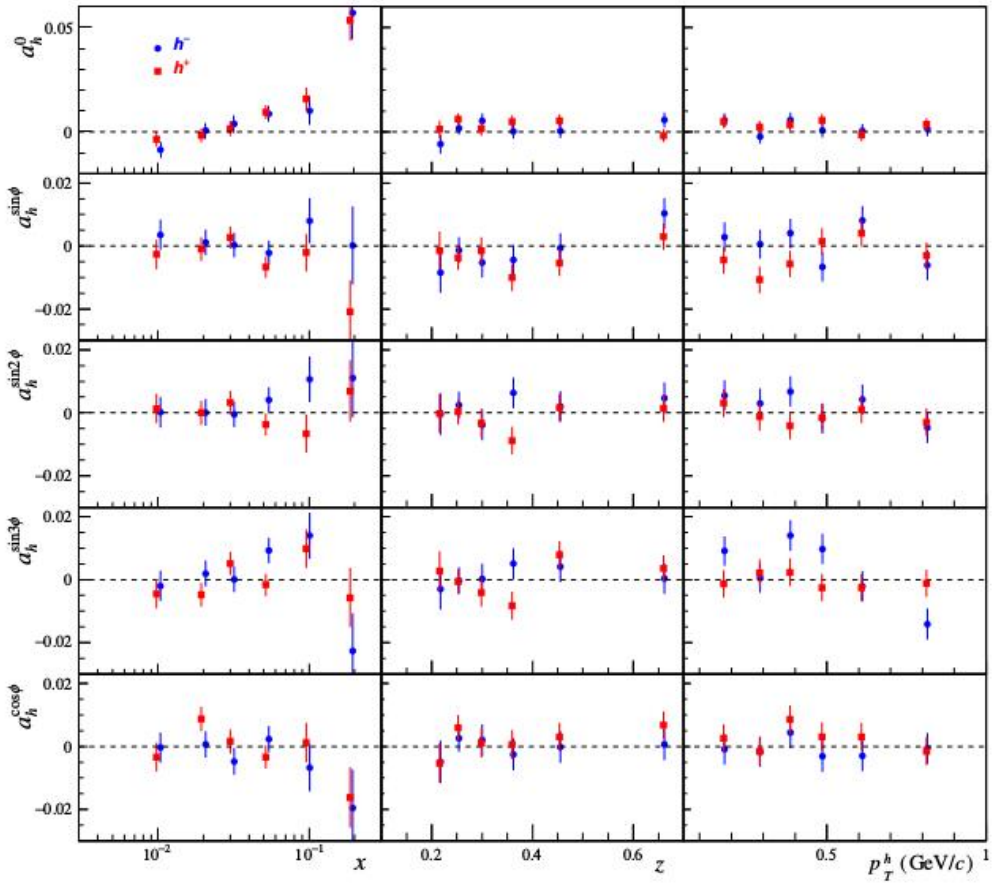

Figure 16:The modulation amplitudes of the h^+ and h^- azimuthal asymmetries as a function of x , z and p_T^h obtained from the combined 2002–2006 data on the muon SIDIS off Longitudinally polarised deuterons.

The amplitudes of the five terms have been first extracted for the data integrated over all kinematic variables. In further fits, the φ-dependence is determined as a function of one of three kinematic variables (Bjorken-x, fractional energy of virtual photon taken by the outgoing hadron and hadron transverse momentum), while disregarding the other two. Except the φ-independent term, all the modulation amplitudes are very small, and no clear kinematic dependence could be observed within experimental uncertainties.

3.5 JINR contribution

For reporting three years of work, JINR made a decisive or essential contribution to obtaining results and preparation of 8 papers of collaboration (see list below). One has be noted a defining contribution of our physicists to alignment of experimental setup, data production and selection of data for the physical analysis.

During 2014-2016 JINR physics have presented 10 talks at the International Conferences and workshops. The annual international workshop on hadron structure and spectroscopy took place in town Suzdal on 18th-20th of May. COMPASS and JINR group were organizers of the event.

The list of papers with JINR contribution:

«Measurement of the charged-pion polarisability», PRL 114 (2015) 062002
«Search for exclusive photoproduction of $Z^{\pm}_{c}$ (3900) at COMPASS», PLB 742 (2015) 330
«Multiplicities of charged pions and unidentified charged hadrons from deep-inelastic scattering of muons off an isoscalar target», PLB 764 (2017) 001
«Multiplicities of charged kaons from deep-inelastic muon scattering off an isoscalar target», PLB 767 (2017) 133
«Azimuthal asymmetries of charged hadrons produced in high-energy muon scattering off longitudinally polarised deuterons», accepted EPJC
«The COMPASS setup for physics with hadron beams», NIMA 779 (2015) 69
«The spin structure function g1p of the proton and a test of the Bjorken sum rule», PLB 753 (2016) 18
«Final COMPASS results on the deuteron spin-dependent structure function g1d and the Bjorken sum rule», CERN-EP/2016-299

In 2014-2015, 3 Master's (K.Gasnikova, E.Mitrofanov and N.Mitrofanov) and one Bachelor's (A.Gridin) degree were defended.

4. COMPASS-II MEASUREMENTS IN 2017-2019

In recent years parton distribution functions have been generalized to contain information not only on the longitudinal but also on the transverse distributions of partons in a fast moving hadron. Eight independent transverse momentum dependent (TMD) parton distributions were identified [1-3] at leading twist, with the transverse momentum k_T of partons included, which are accessible in SIDIS. As shown recently in [4-8], the interaction between the active parton in the hadron and the target spectators leads to the gauge-invariant TMDs. Several reviews have been recently dedicated to theory, phenomenology and experimental measurements of TMD distributions [9-11]. The phase-space Wigner distributions [7] contain most general one-body information of protons. After integration over the spatial coordinates, they reduce to TMDs (see Fig. 17), and after integration over the transverse momentum and a specific Fourier transform they recover the GPDs [12-14].

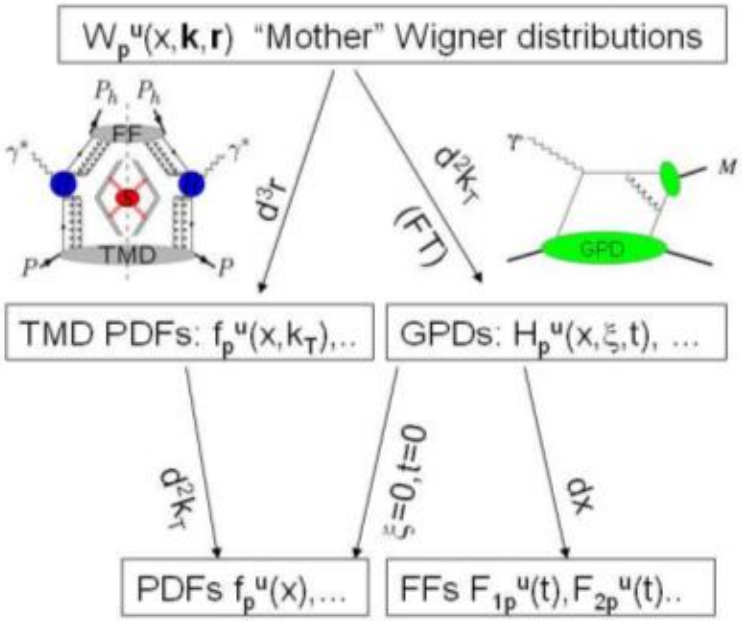

Figure 17: Wigner distributions

Wigner distributions also provide a novel tool to access quark orbital angular momentum [15-18] and their studies in different theoretical models can provide new insights on the quark and gluon dynamics [15-19]. Furthermore, QCD factorization for semi-inclusive deep inelastic scattering at low transverse momentum in the current fragmentation region has been established in [20, 21].

A detailed verification of factorization and the calculations of the relevant factors in the factorization formulas have also been carried out in Ref. [22]. Recently, a complete TMD factorization derivation, in terms of well-defined TMDs with individual evolution properties, was presented by Collins [23]. That formalism has been used to obtain evolved TMDs from fixed-scale fits [24-25]. This new framework provides a rigorous basis to study the TMD parton distributions from the great wealth of existing SIDIS data of different spin-dependent and independent observables.

TMD and GPD distributions (Fig.18) describe partons with certain polarizations in nucleons with another polarization state. The diagonal elements of TMD and GPD tables are the momentum, longitudinal and transverse spin distributions of partons and after integration over transverse degrees of freedom represent the well known PDFs related to the leading-twist light-cone wave functions square: the momentum ($f_1(x, k^2_T)$), the helicity ($g_1(x, k^2_T)$) and the transversity ($h_1(x, k^2_T)$) distributions. They are the only ones that survive after integration over the intrinsic transverse momentum k_T , and are all needed for a complete description of the collinear nucleon structure.

N/q	U	L	T
U	$\mathbf{f_1}$		$h_1^\perp$
L		$\mathbf{g_{1L}}$	$h_{1L}^\perp$
T	$f_{1T}^\perp$	g_{1T}	h_1 , $h_{1T}^\perp$

	U	L	T
U	$\mathcal{H}$		$\mathcal{E}_T$
L		$\widetilde{\mathcal{H}}$	$\widetilde{\mathcal{E}}_T$
T	$\mathcal{E}$	$\widetilde{\mathcal{E}}$	$\mathcal{H}_T$,$\widetilde{\mathcal{H}}_T$

Figure 18: Leading twist TMD distribution functions (left) and GPDs (right). The U,L,T correspond to unpolarized, longitudinally polarized and transversely polarized nucleons (rows) and quarks (columns)

The COMPASS-II measurements have been started in 2012 with pion/kaon polarizability via Primakoff reactions and with GPD feasibility test using partially upgraded COMPASS-II spectrometer. The further measurements were continued in 2014 after the accelerator shutdown. One will be focused on studies of transverse momentum dependent (TMD) distributions of partons in nucleons via Drell-Yan lepton pair production (2014-2015 and in 2018) and measurements and generalized parton distributions (GPDs) via hard exclusive meson production and DVCS (2016-2017) (Fig.19). In parallel with the GPD program, high statistic data for SIDIS will be taken.

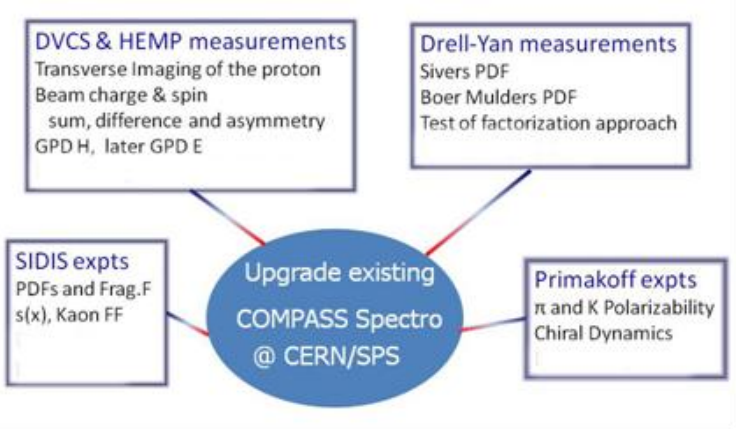

Figure 19: The schematic view of the COMPASS-II measurements for 2012-2018.

4.1 GPD measurements

The GPDs are universal distributions which contain as limiting cases nucleon form factors on the one hand and parton distribution functions (PDFs) on the other. The GPDs H^f and $\tilde{H}^f$ ($f = u, d, s, g$) describe processes where the nucleon helicity is preserved and contain as limiting cases the PDFs f_1 and g_1 , respectively. Processes where the nucleon helicity is flipped are described by the GPDs E^f and $\tilde{E}^f$ for which no such limiting case exists. GPDs correlate transverse spatial and longitudinal momentum and thus provide a kind of `nucleon tomography'. They depend on four variables x, ξ, t, and Q^2. The cleanest process to assess GPDs is DVCS shown in Fig.20, in which also the relevant momentum fractions x (not the Bjorken scaling variable) and ξ, and the momentum transfer t and Q^2 are defined.

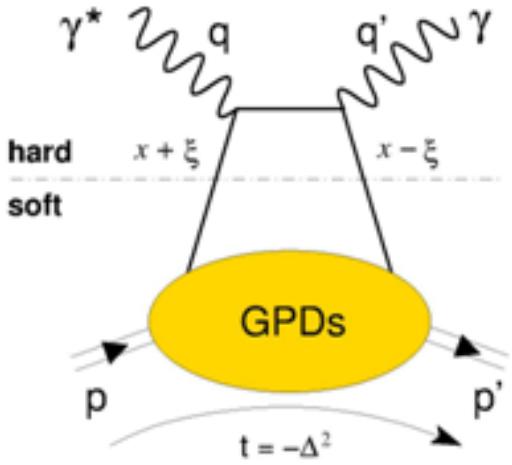

Figure 20: The diagram of the DVCS process.

The interest in these distributions was boosted, when X.¬D. Ji showed that there is a sum rule for the total angular momentum J of a quark or a gluon and the corresponding GPDs [42]. The DVCS process interferes with the Bethe-Heitler (BH) process due to identical final states. The cross-section then contains five terms

$$\mathrm{d}\sigma^{\mu p\to\mu p\gamma} = \mathrm{d}\sigma^{\mathrm{BH}} + \mathrm{d}\sigma_0^{\mathrm{DVCS}} + P_\mu \mathrm{d}\Delta\sigma^{\mathrm{DVCS}} + e_\mu \Re\mathrm{e}\, I + P_\mu e_\mu \Im\mathrm{m}\, I,$$

where I denotes the DVCS-BH interference term. An important feature is that the BH contribution can be normalized at small xB , where it dominates. From above equation one can build the sum S and difference D of the μp -> μpγ cross-section for simultaneous change of lepton charge eμ and polarization P_μ of the incoming lepton beam (+ to - and -> to <-)

$$\mathcal{D} = \mathrm{d}\sigma^{\overleftarrow{+}} - \mathrm{d}\sigma^{\overleftarrow{-}} = 2(\mathrm{d}\sigma_0^{\mathrm{DVCS}} + \Re\mathrm{e}\, I)$$
$$\mathcal{S} = \mathrm{d}\sigma^{\overleftarrow{+}} + \mathrm{d}\sigma^{\overleftarrow{-}} = 2(\mathrm{d}\sigma_0^{\mathrm{BH}} + \mathrm{d}\sigma_0^{\mathrm{DVCS}} + \Im\mathrm{m}\, I)$$

At COMPASS, the DVCS (μ p → μ pγ) will be measured using the high intensity polarized muon beam. DVCS is a relatively low cross section process, so the luminosity will be maximized with a 2.5 meter long liquid hydrogen target. In the DVCS kinematics, the photon is produced at forward angle, and the proton recoils at very large angle. To measure and identify the recoil proton, a 4-meter long Time-Of-Flight detector called CAMERA is surrounding the target. To extend the kinematic coverage of DVCS detection to the higher x_{Bj}, a large angle electromagnetic calorimeter (ECAL0) has also been added. With such an apparatus, COMPASS can measure the DVCS process on a wide x_{Bj} range (from 0.005 to 0.3) with a Q^2 up to 20 GeV^2 (limited by integrated luminosity).

The GPD *H* is studied with DVCS measurements on unpolarized hydrogen. The first proof of principle for the possibility to measure DVCS in COMPASS was brought by a 10-day long run test in 2009 with a reduced setup (40 cm liquid hydrogen target, short recoil proton calorimeter, no additional calorimetry). A pilot run has been recorded in 2012, and the full DVCS run will be recorded in 2016-2017.

In 2012, a four-week long pilot run has been recorded, with a mostly complete DVCS setup (full scale recoil proton detector, full luminosity, partially equipped large angle calorimeter). The analysis of this data is ongoing. The exclusive photon sample selected for data analysis is shown in Fig.21, as a function of $\varphi_{\gamma^*\gamma}$, the azimuthal angle between the leptonic plane (defined by the incident and scattered lepton) and the hadronic plane (defined by the virtual and real photon) are given in 3 following bins in x_{Bj} : $0.005 < x_{Bj} < 0.01$; $0.01 < x_{Bj} < 0.03$; $0.03 < x_{Bj} < 0.27$.

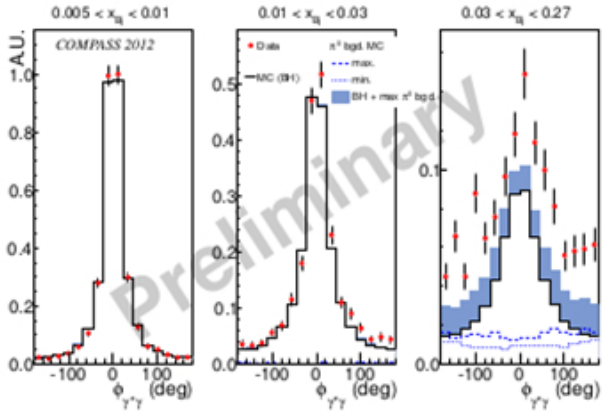

Figure 21: The exclusive single photon events obtained in the 2012 sample as a function of $\varphi_{\gamma^*\gamma}$ (red dots) compared to the Bethe-Heitler estimation (black histogram) and the π_0 contamination estimated by LEPTO and HEPGEN. The visible π_0 background has been subtracted from these data.

The Bethe-Heitler process shares the same final state as DVCS (therefore it interferes with it), but the photon is radiated by the incident or the scattered lepton instead of the proton. The amplitude of the Bethe-Heitler process can be calculated with very good accuracy, and on Figure 21, the Monte-Carlo estimation (black histogram) only includes Bethe-Heitler. In the lower x_{Bj} bin, where the DVCS contribution is negligible, the $\varphi_{\gamma^*\gamma}$ distribution for the data (red dots) agrees remarkably well in shape with the Bethe-Heitler estimation by Monte-Carlo.

The DVCS cross-section depends on the squared momentum transfer t from the initial to final nucleon. At small xBj (X_B) one has the relation

$$\left\langle r_\perp^2(x_B)\right\rangle \approx 2B(x_B),$$

if the exclusive cross-section is parameterized as

$$d\sigma/dt \propto \exp(-B(x_B)|t|).$$

The transverse distance is measured between the struck quark and the centre of mass of the spectator system. Thus, independent of any GPD parameterization, one obtains a measure of the transverse nucleon size as a function of x_B. Using a parameterization of the type,one can characterize the t' slope of the cross-section by the parameter α'. The analysis of the t-slope of the DVCS cross section with this statistics is ongoing. Preliminary results and its comparison with HERA data are shown in Fig.22.

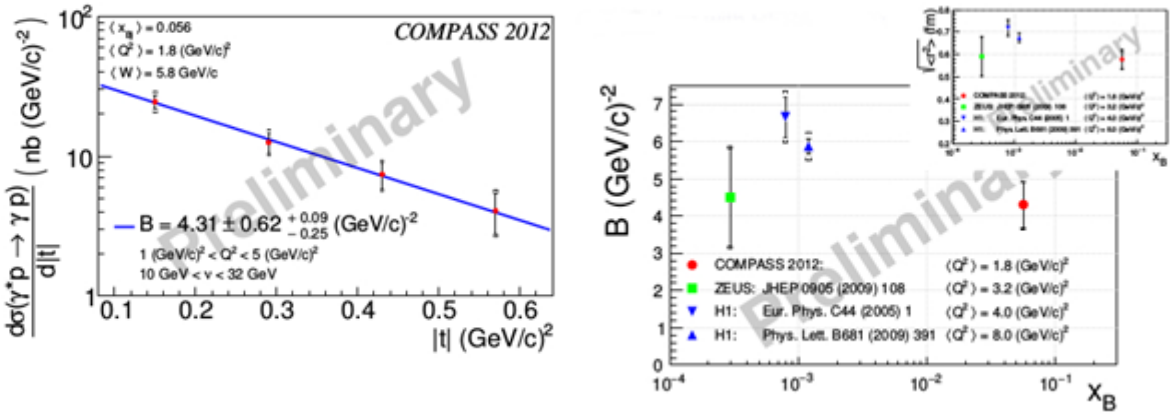

Figure 22: DVCS cross section and t-slope extraction (left panel). Comparison on B and <r2> with HERA results (right panel)

4.2 Drell-Yan measurements

Due to their naive time reversal odd nature, Sivers and Boer-Mulders TMD PDFs change sign when accessed from DY or from SIDIS. The experimental observation of this sign-change is considered a crucial test of the TMD approach of non-perturbative QCD. The Drell–Yan quark–antiquark annihilation process is an excellent tool to study transversity and kT -dependent T -odd PDFs. In the DY process (Fig. 11) quark and antiquark annihilate into a lepton pair. Other kinds of hard processes can also access chirally odd PDFs, like semi-inclusive deep-inelastic scattering (SIDIS) where chirality is conserved through the convolution of PDFs with polarised quark fragmentation functions. There exist no fragmentation process in DY. In order to access spin structure information a high-intensity hadron beam and a large-acceptance set-up as well as a high-performance polarised target are required. These features are provided by the multipurpose large acceptance Compass spectrometer in combination with the SPS M2 secondary beam line and the large-acceptance polarised target. In more detail, the Compass experiment is characterised by the availability of:
– a transversely polarised solid-state proton target with a high polarisation and a long relaxation time in frozen-spin mode,
– intense secondary hadron beams of intensities up to 109 hadrons/spill,
– a detection system designed to stand high particle fluxes.
The analysis of data taken in 2015 is in progress.
The estimated uncertainties on asymmetries described in chapter 3.3 are given in Fig.23.

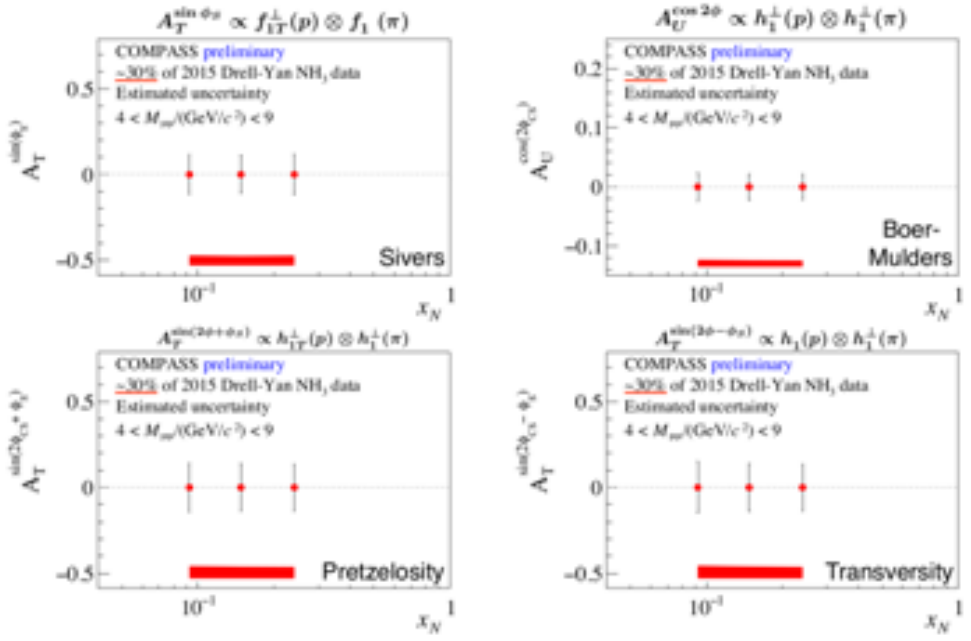

Figure 23: The estimated uncertainties on asymmetries (details are given in chapter 3.3) from 2015 data.

Currently COMPASS has proposed DY measurements for 2018 run. In case of approval of this proposal by SPSC CERN committee, the DY statistics will be increased essentially. As example, Fig.24 presents the possible projection for Sivers asymmetry with prediction in the assumption that PDFs sign will change in DY and SIDIS processes.

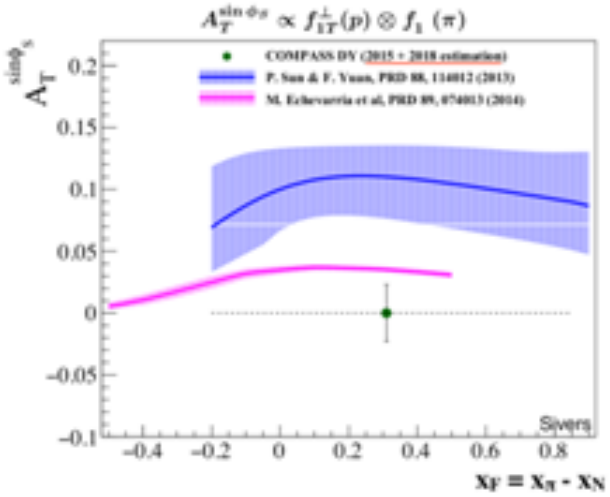

Figure 24: The projection of Sivers asymmetry in DY measurements for 2015 and 2018 data taking.

4.3 SIDIS studies.

High-statistics data on semi-inclusive deep inelastic scattering (SIDIS) on the proton, μp→μhX, will be taken simultaneously with the DVCS and HEMP measurements using the long liquid hydrogen target. Combined with existing SIDIS data on the deuteron, they will permit to improve precision of unpolarized quark flavour distributions. The new proton data will be obtained in a region of Bjorken-*x* (denoted by *x* in the rest of this section), where measurements from other experiments are either not available or have limited precision. The new data will be used in global QCD analyses to constrain structure functions of unpolarized nucleons. They permit also to improve measurements of quark Fragmentation Functions (FFs), which describe quark fragmentations into hadrons. The latter functions are necessary also for determination of polarized parton distributions. Presently, FFs are still poorly known quantities introducing large systematic uncertainties in determinations of parton distributions in nucleons, particularly in distributions of strange quarks. The new data will permit determination of the unpolarized strange quark distribution function *s(x)* in the region $0.001 < x < 0.2$, where its shape is unknown. In addition, using the same data, it will be possible to measure with high statistics asymmetries in the azimuthal distributions of hadrons produced in SIDIS on an unpolarized proton target. These measurements, already performed with deuteron target, are sensitive to the T-odd transverse-momentum-dependent (TMD) Boer–Mulders function [43] and also to the Cahn effect [44], both depending on the intrinsic transverse momentum of quarks k_T .

4.4 JINR activities.

As it was mentioned in chapters 2.4-2.6, the JINR group is obliged to support 3 detectors: HCAL1, MW1 and ECAL0 during 2017 data taking , and two detectors (MW1 and HCAL1) – for 2018 data taking. Also DAQ system is under support form JINR group (V.Frolov). JINR participates in the preparation and support of the polarised target (Yu.Kiselev) and hall engineering (V.Anosov). Detailed information on JINR tasks is also given in section 6.

5. COMPASS-II ANALYSIS IN 2017-2019

5.1 Primakoff reactions with 2009 and 2012 data

5.1.1 Pion and kaon polarizabilities

In spite of the precise result for pion polarizabilities obtained by COMPASS its uncertainty is still much larger than the accuracy of the ChPT prediction. A new set of data collected at COMPASS during the hadron run 2012 with a few times larger statistics is under analysis. The statistics in the control sample collected with a muon beam in 2012 was also increased. Therefore, one can expect reduction of both statistical and systematic uncertainties of the new result for $\alpha\ \pi$ under assumption $\alpha_\pi+\beta_\pi=0$. The new data cover a larger range of the photon energy in respect to 2009, down to about 20 GeV, that is especially important for independent measurement of α_π and β_π. Since the kaon is a more compact and rigid object than the pion, it would be natural to expect smaller values for kaon polarizabilities. The prediction of the chiral perturbation states that, for the charged kaon, the polarizability is $\alpha_K=(0.64\pm0.10)\times10^{-4}$ fm^3 under assumption that $\alpha_K+\beta_K=0$ [45]. While the prediction of the quark confinement model is rather different: $\alpha_K=2.3\times10^{-4}$ fm^3, $\alpha_K+\beta_K=1.0\times10^{-4}$fm^3 [46]. As for the experimental results, only the upper limit $\alpha_K<200\times10^{-4}$ fm^3 (CL=90%) has been established from the analysis of X-rays spectra of kaonic atoms. The reaction

$$K^-(A, Z) \rightarrow K^-(A, Z)\gamma. \quad (10)$$

can be used to determine the kaon polarizability. The expected ratio *R* for the kaon with polarizability $\alpha_K=0.6\times10^{-4}$fm^3 and for the pion with polarizability $\alpha_\pi=2.8\times10^{-4}$fm^3 as a function of x_γ is depicted in Fig.25 (left). Despite small contamination of kaons in the beam and low cross section of the reaction (10) (proportional to m^{-2}) COMPASS provides unique possibility to touch this quantity.

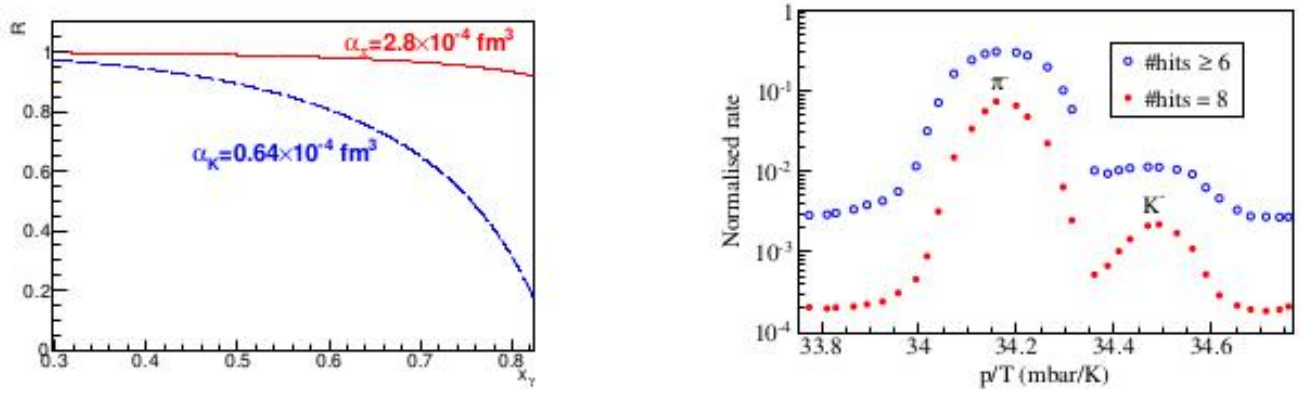

Figure 25: Ratio R of the differential cross sections for the pion with polarizability απ=2.8×10−4 fm3 and the kaon with polarizability αK=0.64×10−4 fm3 to the corresponding cross sections for the point-like pion and kaon (left). π/K identification by the CEDARs in the COMPASS negative hadron beam (right).

COMPASS capability to identify beam hadron is shown in Fig. 25 (right).

5.1.2 Pion electromagnetic reactions with pions in the final state

In parallel to the pion and kaon polarizabilities measurements COMPASS also aims to study low Q^2 electromagnetic reactions with mesons in the final state:

$$\pi^-(A, Z) \rightarrow \pi^-(A, Z)\,\pi^0, \quad (8)$$

$$\pi^-(A, Z) \rightarrow \pi^-(A, Z)\,\pi^+\pi^-, \quad (9)$$

$$\pi^-(A, Z) \rightarrow \pi^-(A, Z)\,\pi^0\,\pi^0. \quad (10)$$

The measurement of Eq. (8) allows determining the chiral anomaly amplitude $F_{3\pi}$, for which the ChPT makes an accurate prediction by relating the process to the π^0 decay constant F_π [47]:

$$F_{3\pi}(s=0,t=0,Q^2=0)=\frac{F_\pi}{f^2\sqrt{4\pi\alpha}}, \tag{11}$$

where f is the the charged pion decay constant. This constitutes a test of a higher-order ChPT predictions. The reaction has already been examined at the SYGMA spectrometer (Serpukhov), however in the relevant region of s<10m2π only about 200 events were found. The constant of the similar reaction with η-meson in the final state has been also tested in VES experiment (Serpukhov) with low precision. The cross sections of the reactions (9) and (10), which are governed by the chiral ππ-interaction, calculated as functions of the center-of-mass energy √s at the tree level in [48], are shown in Fig. 26 (left). Here, the ChPT expansion should be reliable on the percent level, and thus, the experiment would constitute a strong test of ChPT at the tree level and much beyond the determination of low-energy constants. The cross section of the reaction (10) has already been measured as a function of √s by COMPASS [49] and is in good agreement with the ChPT prediction. Preliminary result for π-$\pi^0\pi^0$ mass spectrum for events with small 4-momentum transferred to nucleus obtained using 2019 data is shown in Fig. 26 (right).

Similar kaon-induced reactions can also be tested in COMPASS.

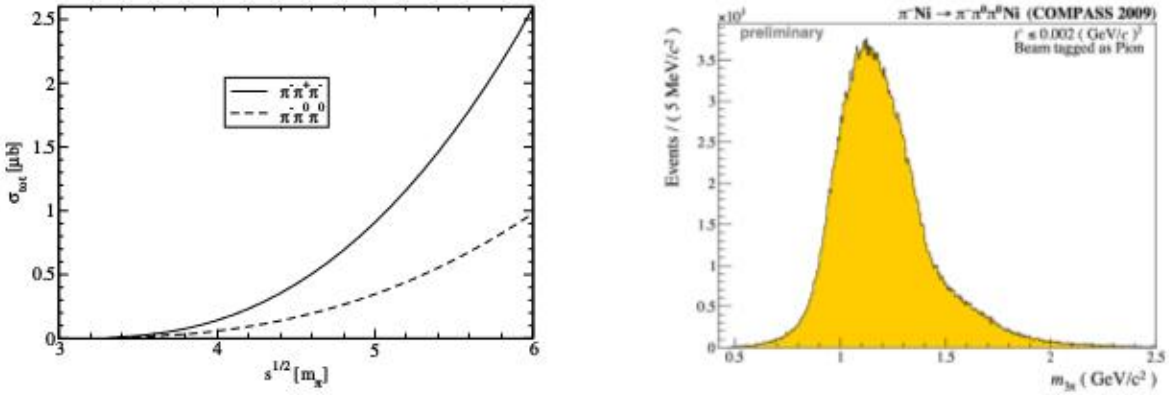

Figure 26: Total cross sections for the reactions (9) and (10) as a function of the total center-of-mass energy √s (left) [4]. Mass spectrum of π−π0π0 state for events with small 4-momentum transferred to nucleus (2009 data, preliminary result).

5.2 Drell-Yan studies

5. 2.1 Study of the EMC effect in the pion-induced Drell-Yan process.

The momentum distribution functions of the partons within the hadron ($q(x,Q^2)$, $\bar{q}(x,Q^2)$,$g(x,Q^2)$,called Parton Distribution Functions (PDFs) are the main instrument to describe the structure of hadrons in the quark-parton model. They represent the probability densities to find a parton carrying a momentum fraction *x* at a squared energy scale Q^2.

The EMC effect - a modification of quark and gluon distributions in bound nucleons by the nuclearenvironment was discovered by the European Muon Collaboration in 1983 in the deep inelastic scattering of muons. Since then the EMC effect has been observed in the numerous experiments. The dependences of nuclear modifications of the parton distributions on kinematics and various nuclear properties likemass, density or radius of a nucleus are rather well-known, but, nevertheless, the origin of the effects still not fully understood. Numerous explanations of the EMC effect have been proposed: nuclear binding, pion excess in nuclei, multi-quark clusters, dynamical rescaling, medium modification, short-range correlations, CBT model, etc. However, there is no generally accepted model for the effect over all *A* and *x*.

Despite the DIS being the main instrument to study the EMC-effect, the effect has also been experimentally verified in the time-like region using both the pion- and the proton-induced Drell-Yan reactions in the E772, E866, NA3, and NA10. In the Drell-Yan process a quark (anti-quark) with the momentum fraction x_1 from the beam hadron and an anti-quark (quark) of the target nucleon with the momentum fraction x_2 annihilate via a virtual photon into a charged-lepton pair: q(x_1) q-bar (x_2)→γ^* l^+l^- . The invariant mass of the produced pair is:

$$M_{l^+l^-} = \sqrt{x_1 x_2 s}, \tag{12}$$

where s is the nucleon-nucleon center-of-mass energy. The Drell-Yan cross section is

$$\frac{d^2\sigma_{DY}}{dx_1 dx_2} = K\frac{4\pi\alpha^2}{9x_1x_2}\frac{1}{s}\sum_{q=u,d,s\ldots} e_q^2\left[q(x_1)\bar{q}(x_2) + \bar{q}(x_1)q(x_2)\right]. \tag{13}$$

K≈2 is a factor representing the deviation from the simple parton model due to QCD corrections.

The pion-induced Drell-Yan process is complementary to the DIS process and can provide another experimental tool that is sensitive to flavor-dependent effects in the nuclear quark distributions [26] (since in the DIS contributions of u and d quarks are mixed). Keeping only the dominant terms in the cross section, one readily obtains

$$\frac{\sigma_{DY}^{\pi^- A}}{\sigma_{DY}^{\pi^- D}} \approx \frac{u_A(x_2)}{4u_D(x_2)}, \tag{14}$$

where $u_A(x_2)$ and $u_D(x_2)$ are PDFs for u-quark in a nucleus with a mass A and deuterium, respectively.

The previous measurements of a nuclear dependence of the pion-induced Drell-Yan cross section have been performed in the experiments NA3 and NA10 for tungsten and deuterium targets using a negative pion beam of 140 GeV/c and 286 GeV/c in the dilepton mass range above 4.35 GeV and 4.2 GeV, respectively. The accuracy was enough to confirm the observation of the EMC effect, but it is too low for detailed tests of various theoretical models.

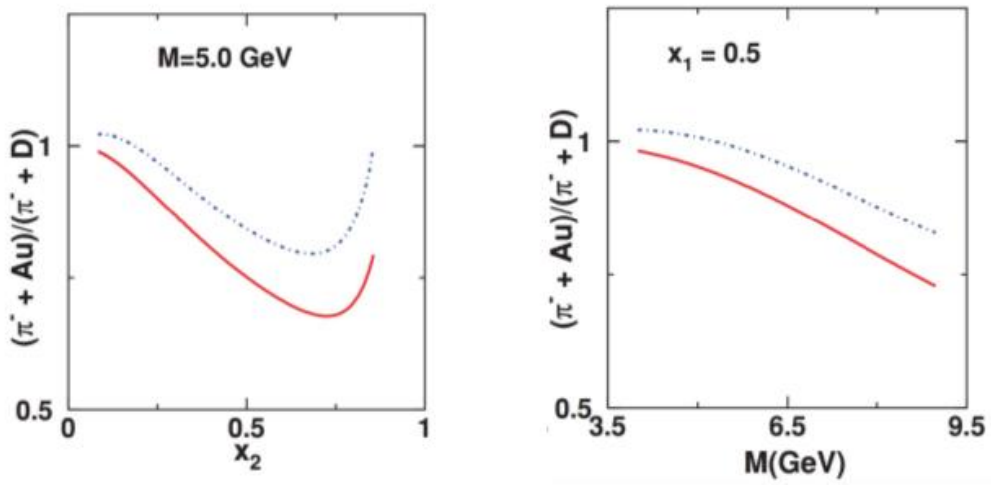

Figure 27: Ratio of the Drell-Yan cross sections for Au and D calculated for the COMPASS kinematic coverage using the PDFs from the CBT model as a function of x 2 for the fixed mass M l + l − =5 GeV (left) and as a function of M l + l − for the fixed value x1 = 0.5 [28].

The ratio (14) of the cross sections calculated for the COMPASS kinematic coverage using the PDFs for deuterium and gold from the CBT model is presented in Fig.27 as a function of x_2 for the fixed mass $M_{l^+l^-}$ =5 GeV (left) and as a function of $M_{l^+l^-}$ for the fixed value x_1 = 0.5.

Data taking for the Drell-Yan process study with a negative pion beam of 190 GeV/c (√s=18.9 GeV) was performed at COMPASS in 2014 and 2015. The main ammonia target, the tungsten beam plug of the hadron absorber and an additional aluminium target can be used to study the EMC effect. The expected statistics for Drell-Yan dimuon pairs is much higher than in the previous similar experiments such as NA3 and NA10. The kinematic range of x_1 and x_2 for Mμμ > 4 GeV covered by COMPASS for the ammonia target is shown in the left and right panels of Fig.28, respectively. Dimuon mass resolution for J/ψ peak is about 0.2 MeV for the ammonia, while for the tungsten plug it is a bit worse. Thus, to be save, only the mass range above 5 GeV can be used for investigation of the EMC effect, which defines, according to Eq. 12, a lower limit of x_2 range accessible by COMPASS to be 0.07.

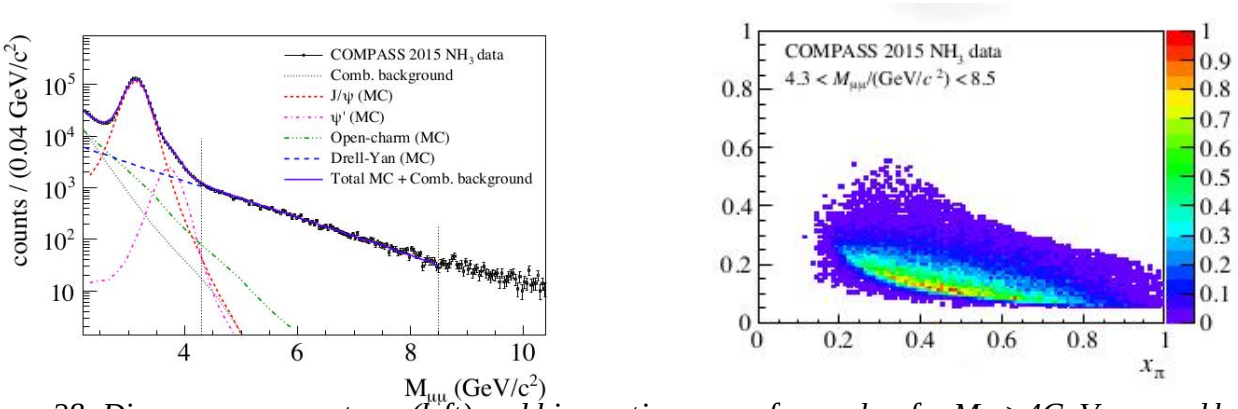

Figure 28: Dimuon mass spectrum (left) and kinematic range of x_1 and x_2 for $M_{\mu\mu}$>4GeV covered by COMPASS (right) for the ammonia target.

Study of nuclear effects in charmonia production could also be performed at COMPASS. Since the gluon fusion gg → J/ψ is a significant part of the J/ψ production mechanism in hadron collisions, comparison of the cross sections of J/ψ production for ammonia, aluminium and tungsten provides access to the EMC effect for gluons.

5.3 Exotic charmonia

The exotic hadron X(3872) was first discovered in 2003 by the Belle collaboration and constitutes the first in a long series of new charmonium-like hadrons at masses above 3.8 GeV/c^2. The mass of the X(3872) has been determined to be 3871.69±0.17 MeV/c^2, which is very close to the D^0D^{*0}-bar threshold. However, now the decay width of this state could not be determined yet as the observed width has been compatible with the experimental resolution in all experiments. Thus, only an upper limit for the natural width $\Gamma_{X(3872)}$ of about 1.2 MeV/c 2 (CL=90%) exists. The quantum numbers J^{PC} of the X(3872) have been determined by LHCb to be 1^{++}. The X(3872) hadron is peculiar in several aspects and its nature is still not well-understood. Approximately equal probabilities to decay into J/ψ2π and J/ψ3π final states (B (X(3872) → J/ψω)/ B (X(3872) → J/ψπ^+ π^-) = 0.8 ± 0.3) indicate large isospin symmetry breaking.

The first glimpse of the X(3872) lepto-production at COMPASS is observed in the exclusive reaction

$$\mu^+ N \to \mu^+ X^0 \pi^\pm N' \to \mu^+ (J/\psi \pi^+ \pi^-) \pi^\pm N' \to \mu^+ (\mu^+ \mu^- \pi^+ \pi^-) \pi^\pm N',$$

where X^0 is the well-known charmonium ψ(2S) or the exotic state X(3872). Preliminary result for the mass spectrum of the J/ψ$\pi^+\pi^-$ subsystem is depicted in Fig.29 (right). It exhibits two resonant structures for M<4 GeV with a statistical significance of about 5σ, which can be assigned to the production and decay of ψ(2S) and X(3872). Measurement of absolute production rate of X(3872) in the reaction (15) could provide important input for clarification of its nature. Search for another exotic charmonia in J/ψφ, J/ψ$\pi^+\pi^-\pi^\pm$, ψ(2S)$\pi^\pm$, ψ(2S)$\pi^+\pi^-$ final states is ongoing.

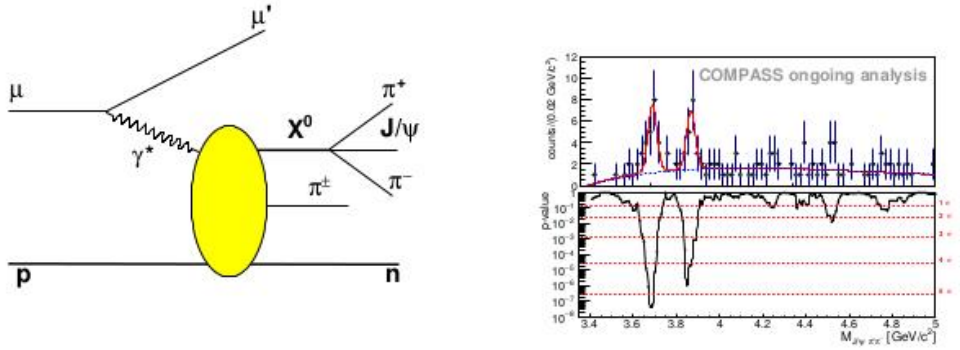

Figure 29: Schematic diagram for X(3872) photoproduction off a nucleon (left). Mass spectrum for the J/ψπ + π− subsystem (right)

Upgrade of the COMPASS setup for the GPD programme (2016-2017) provides new opportunities for searching for leptoproduction of exotic charmonium-like states. The system of electromagnetic calorimeters ECAL1 and ECAL2 has been extended by installing a new large-aperture calorimeter ECAL0. With the new calorimetry system one can expect much better selection of exclusive events. Searching for the production of exotic charmonia decaying into the final states with π^0, η and χ_c -mesons, which decays into $J/\psi\gamma$, could also be possible. Absence of neutrons in the new hydrogen target in combination with the recoil proton detector CAMERA, which can be used for reconstruction of a recoil proton in the reactions with neutral exchange and as a veto for the reactions with positive charge exchange, also improves the quality of exclusive events selection and background suppression.

The exotic states $P_c^+(4380)$ and $P_c^+(4450)$ have been observed by the LHCb collaboration in the $J/\psi pcuud$, and thus are mass spectrum in the decay $\Lambda_b^0 \rightarrow J/\psi pK^-$. They must have minimal quark content c^- good candidates to be exotic hidden-charm pentaquarks. Search for exclusive photoproduction of these states in the reaction

$$\gamma p \rightarrow J/\psi p \qquad (15)$$

is proposed in [50, 51]. The dominant contribution to the cross section of this reaction is the diffractive process, which can be accounted by the Pomeron exchange in the t-channel, while the excitation of $P_c^+(4380)$ and $P_c^+(4450)$ can occur mainly via the s-channel. In 2002-2011 muon data the corresponding kinematic range was not covered by the trigger, only the events with $\sqrt{s_{\gamma p}} > 6$ GeV were accepted. But exclusive leptoproduction of the states $P_c^+(4380)$ and $P_c^+(4450)$ potentially can be searched for in the future COMPASS muon runs in the reaction:

$$\mu^+ p \rightarrow \mu^+ P_c \rightarrow \mu^+ J/\psi p \rightarrow \mu^+ \mu^+ \mu^- p. \qquad (16)$$

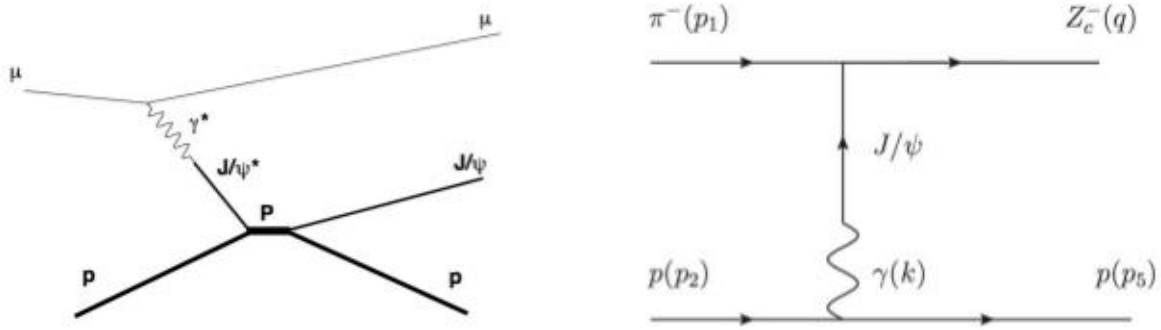

Figure 30: Diagram for Pc+ states leptoproduction in the reaction (16) (left). Diagram for Z_c^- state production in the reaction the reaction (16) (right).

The possibility to exclusively produce the charmonium-like state $Z_c^{\pm}(3900)$ in the pion-induced reaction off a nuclear target (see Fig. 30 (left)) is discussed in [52,53]. The $Z_c^{\pm}(3900)$ can be produced by interaction of a high-energy pion beam with the Coulomb field of a nucleus:

$$\pi^-(A,Z) \rightarrow Z_c^-(3900)(A,Z) \rightarrow J/\psi\pi^-(A,Z). \qquad (17)$$

The dependence of the cross section of this reaction on the atomic number of a nucleus is defined by the strength of the Coulomb field that is proportional to Z^2 and by the electromagnetic form factor of a nucleus and grows rapidly with an increasing charge of a nucleus. The production mechanism mentioned above can be tested using the Drell-Yan data collected with a 190 GeV/c negative pion beam of high intensity in 2014-2015. Since the beam plug is installed, the DY setup is transparent for muons only and the possible decay $Z_c^-(3900) \rightarrow J/\psi\pi^-$ cannot be observed directly. But the fact of the $Z_c^-(3900)$ production via the reaction (18) can be tested by comparison of the momentum spectra of J/ψ produced in the ammonia target, thin aluminium

target and the tungsten plug. The energy transferred to the target nucleus is law while the energy of the produced $Z_c^-(3900)$ is about the energy of the beam. Due to the huge mass asymmetry between the decay products of $Z_c^-(3900)$, J/ψ and π^- , the produced J/ψ should have flat energy distribution starting from about $E_0 m_{J/\psi}^2 / m_{Zc(3900)}^2 \approx 120$ GeV, where E_0=190 GeV is the pion beam energy. Since the $Z_c^-(3900)$ production cross section off tungsten is expected to be much larger than off the proton or nitrogen, an excess of energetic J/ψ-mesons from the tungsten plug may indicate the production mechanism.

5.4 SIDIS reactions

The studies of SIDIS (Semi-Inclusive Deep Inelastic Scattering) reactions is the one of most advanced task of COMPASS-II physics program. The set analyses were performed yet with SIDIS data taken in 2002-2010 (see refs from Appendix 11, 23-26,31.32,45,49,51):

• Studies of transversity distributions:

-Collins asymmetry were measured with polarized deuteron and proton targets in reactions with h±, π± , and K± productions;

- The distributions and asymmetries were studied with polarized proton and deuteron targets in reaction with di-hadron productions(h± , π± , K±);

- The interplay between Collins and di-hadron asymmetries were investigated;

• Studies of TMD PDFs

- Sivers asymmetries were measured;

- The 6 (transverse single asymmetry) TSA were studied with polarized deuteron and proton targets in reactions with only charged hadrons and separately in h± , π±, K± productions;

- Gluon Sivers asymmetry from J/Psi and high p_T hadron pair production were measured on transversely polarised deuteron and proton targets;

- The azimuthal asymmetries were studied on unpolarized deuteron target in reactions h± production.

• Studies of various hadron multiplicities

- Investigations of multiplisities in reactions with single hadron production versus p_T^2 on deuteron target;

– Studies of multiplisities in reactions with 2 hadrons production.

Below one can see the some results on pion multiplicities obtained by COMPASS with active participation of JINR physicists [54-56]. In Figures 31 and 32, the results for the z and y dependences of the π^+ and π^- multiplicities are presented in the nine bins of x. Only statistical uncertainties are shown, which are in most cases smaller than the size of the symbols.

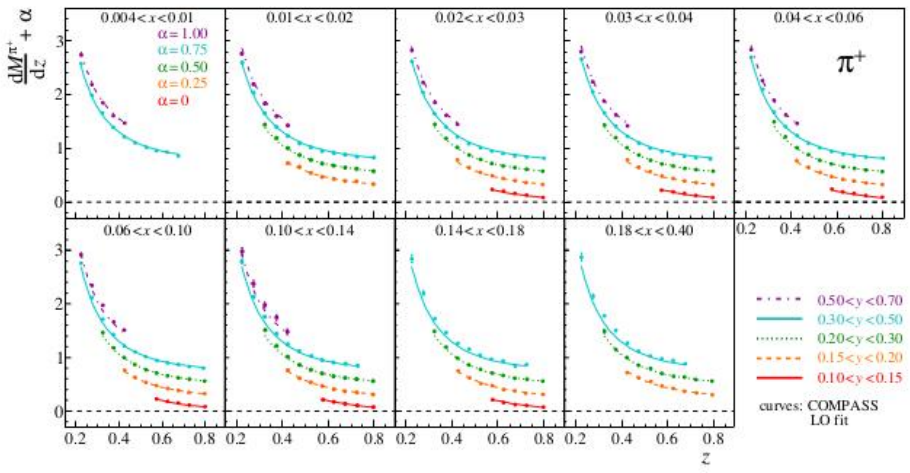

Figure 29. Positive pion multiplicities versus z for nine x bins and five y bins. Only statistical uncertainties are shown. The curves correspond to the COMPASS LO fit.

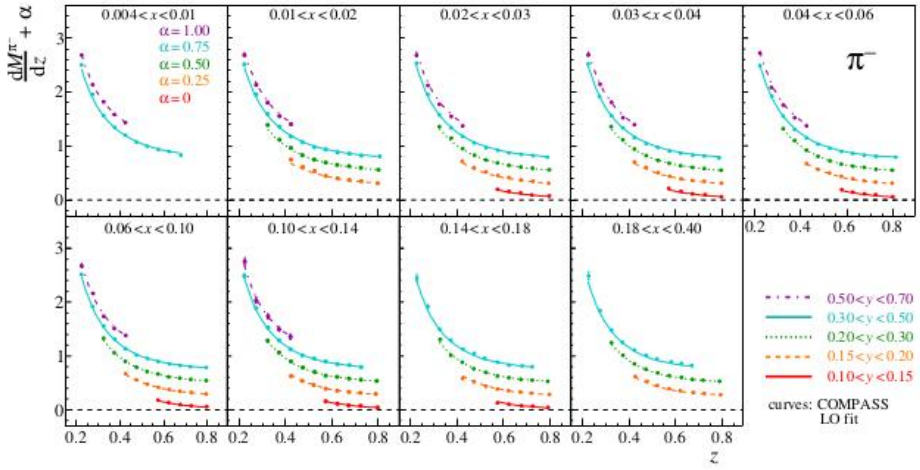

Figure 30. Same as Fig. 29 for negative pions.

Figure 31 (left) shows the result for the sum $M^{\pi+}$ $M^{\pi-}$ of π^+ and π^- multiplicities, integrated over z from 0.2 to 0.85 and averaged over y between 0.1 and 0.7, as a function of x. The expected weak x dependence is indeed observed in the data. In the same figure, the results of HERMES [57] integrated over z from 0.2 to 0.8 are shown using the so-called x representation. The HERMES multiplicities are larger and show a different dependence on x. Note however that the HERMES data were measured at a lower energy and correspond to different kinematics. In order to compare the COMPASS results also with the EMC ones [58], the sum of unidentified-charged-hadron multiplicities is shown in Fig. 31 (right). The results from COMPASS and EMC, which correspond to comparable kinematics, are found in excellent agreement.

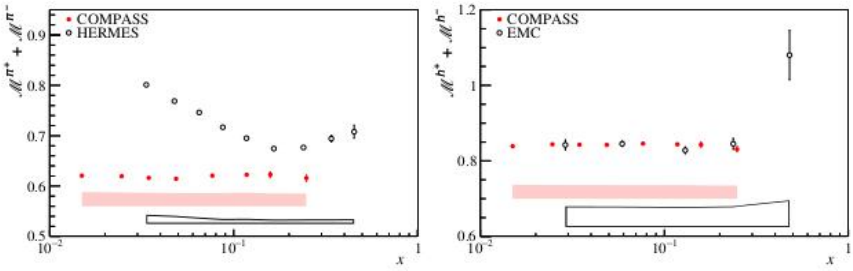

Figure 31: Left: Sum of $M^{\pi+}$ and $M^{\pi-}$ versus x. The COMPASS data (closed circles) are compared to HERMES results (open circles). The systematic uncertainties are shown as bands at the bottom.

Currently many important results produced by COMPASS to investigate transversity and TMDs in SIDIS, but higher statistics data on transversely polarised d data still needed. One expected that more results coming soon from already collected data:

- with transversely polarised proton target - on weighted asymmetries, p_T and Bessel distributions;
- with unpolarised deuteron target- on azimuthal asymmetries, two hadron multiplicities.
- with 2014-2015 data – for transversely polarized DY (sign test).

Also above mentioned analyses will be continued with the new data taken in 2016-2017 using unpolarised proton target (in parallel with DVCS).

5.5 GPD studies

The GPD run has started in 2016 and will be continued in 2017. The first preliminary results are expected to be presented soon. The main tasks of GPDs investigations with Hard Exclusive Photon and Meson Production are as follows:

- measurements of the t-slope of the DVCS and HEMP cross section (transverse distribution of partons);
- studies of the beam-charge-and-spin sum and difference amplitudes (Re (TDVCS) and Im TDVCS for the GPD H determination);
- measurements of longitudinal contribution of Vector Mesons ρ0,ρ+,ω, Φ (GPD H);
- measurement of contributions sensitive to transverse nucleon(parton) polarization (GPDs E, E_T).

The projected precision of a t-slope measurements for two year of data taking is presented in Fig.32.

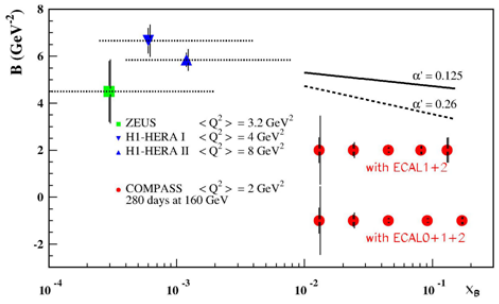

Figure 32: Projected measurements of the xB dependence of the t¬slope parameter B(x_B) (red filled dots) using only ECAL1 and ECAL2 (upper row) and with an additional ECAL0 calorimeter (lower row).

With an unpolarized target, DVCS results will mainly provide information on the GPD H. The projected precision in one of bin is shown in Fig.33 for the beam charge and spin asymmetry.

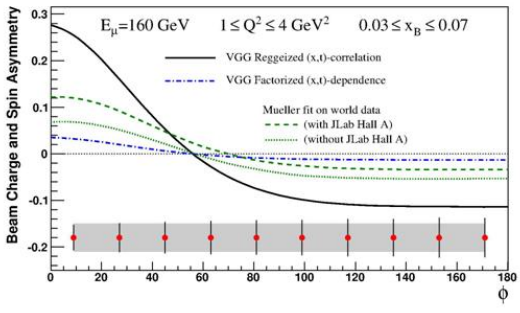

Figure 33: Projected precision of the beam charge¬ and ¬spin asymmetry measurements compared to various models.

6. MANPOWER AND ACTIVITIES.

According to the recommendations of 46th session of PAC, the detailed information on JINR participations and their tasks are presented in this section. The total number of JINR participants are equal to 49, the list is given in table below, one consists of 25 scientists, 11 PhD students (marked as «PhD st» in table below), one diploma student and 12 technicians and engineers. The number of COMPASS author is equal to 18 scientists and 6 PhD students (table below, marked in bolt). The list of physics analyses to be performed in 2017-2019 are as follows:

1.SIDIS,

The participants are Zemlyanichkina E., Mitrofanov N., Ivanshin Yu., Efremov A., Savin I., Ivanov A.

Expected list of the collaboration papers with contributions from above mentiond physicists are:

«Azimuthal asymmetries of charged hadrons produced in high-energy muon scattering off longitudinally polarised deuterons»,

«Multiplicities of charged pions and kaons»,

«Longitudinal spin dependent single-hadron asymmetries»

2. GPD asymmetries,

The participants are Kouznetsov O., Akhunzyanov R., Batozskaya V., Gushterski R., Rogacheva N. and Salmina E. Data analysis just started with 2016 data, currently the main tasks are data selection and preliminary analysis. The work is in progress.

3. Drell-Yan asymmetries,

Currently just Ivanov A. works on that topic, on data selection and Monte-Carlo studies.

4. Pion polarizability

The participants are A.Guskov, Maltsev A., Mitrofanov Ye., Rymbekova A. The analysis of the 2012 data is in progress. The paper drafts are expected soon.

5. Pion electromagnetic reactions with pions in the final state,

The participants are A.Guskov, Gridin A., Denisenko I., Maltsev A., Mitrofanov Ye., Rymbekova A. The data taken in 2009 and 2012 are under analysis.

The paper is expected later 2017.

6. EMC effect in the pion-induced Drell-Yan process

The participants are A. Guskov, Gridin A., Denisenko I., Maltsev A., Mitrofanov Ye., Rymbekova A. The analysis is in progress. The preliminary results are obtained. The paper draft is expected soon.

7. Exotic charmonia

The participants are A.Guskov, Gridin A., Denisenko I. The first set of results are published. The further analysis is in progress.

8. Data production and alignment

The participants are Zemlyanichkina E., Mitrofanov N. These tasks are very important for data analysis, which are are continuously performed.

The technical maintenance of three detectors is a one of the main tasks during data taking. The calorimetry group, which support two calorimeters(HCAl1 and ECAL0), consists of Anfimov N., Antoshkin A., Gavrishchuk O., Meshcheryakov G., Selyunin A., Rezinko T., Rybnikov A., Chirikov-Zorin I., Yukaev A. The second hardware group from LNP, supporting MW1, are as follows: Abazov V.A., Alexeev G., Jouravlev N., Piskun A., Tokmenin V., Golovanov A.

The sum of FTE for LNP is equal to 15.5, for LHEP -12.1, for LTP - 0.6. The total sum of FTE is 28.2 (who are marked by * temporarily do not work in our group).

No.	Name	Status	Activity	FTE	Laboratory
1	Abazov V.	scient	MW1	0,5	LNP
2	Arbuzov A.	scient	Data analysis	0,1	LTP
3	**Alexeev G.**	scient	MW1	0,5	LNP
4	**Anfimov N.**	scient	ECAL0	0,5	LNP
5	**Anosov V.**	tech	Hall Engeneering	1,0	LHEP
6	**Antoshkin A.**	PhD st	ECAL0	0,5	LNP
7	Astakhov V.	tech	ECAL0 electronics	0,1	LHEP
8	**Akhunzyanov R.**	PhD st	Data analysis	1,0	LHEP
9	Batozskaya V.	PhD st	Data analysis	1,0	LHEP*
10	**Gavrishchuk O.**	scient	HCAL1, ECAL0	0,4	LHEP
11	Gridin A.	PhD st	Data analysis	0,5	LNP
12	Gromov V.	tech	ECAL0, Slow control	0,5	LNP
13	**Guskov A.**	scient	ECAL0, Data analysis	0,5	LNP
14	Gushterski R.	scient	Data analysis	1,0	LHEP
15	Denisenko I.	PhD st	Data analysis	0,5	LNP
16	**Efremov A.**	scient	Data analysis, Theory	0,5	LTP
17	**Jouravlev N.**	scient	MW1	0,5	LNP
18	**Zemlyanichkina E.**	scient	Data analysis	1,0	LHEP
19	Ivanov A.	scient	Data analysis	1,0	LHEP*
20	**Ivanshin Yu.**	scient	Data analysis	1,0	LHEP
21	**Kisselev Yu.**	scient	Polarised target	1,0	LHEP
22	**Kouznetsov O.**	scient	Data analysis	1,0	LHEP
23	Maltsev A.	Dip.student	Data analysis	0,5	LNP
24	Golovanov A.	tech	MW1	0,5	LNP
25	**Meshcheryakov G.**	scient	HCAL1, ECAL0	1,0	LHEP
26	**Mitrofanov Ye.**	PhD st	Data analysis	1,0	LNP
27	**Mitrofanov N.**	PhD st	Data analysis	1,0	LHEP
28	**Nagaytsev A.**	scient	Team leader,ECAL0	1,0	LHEP
29	Nikitin M.	tech	ECAL0	0,5	LNP
30	**Olchevski A.**	scient	ECAL0, data analysis	0,1	LNP
31	**Peshekhonov D.**	scient	Data taking	0,5	LHEP
32	Piskun A.	tech	MW1	0,5	LNP
33	Rezinko T.	tech	ECAL0	0,5	LNP
34	Rogacheva N.	scient	Data analysis	1.0	LHEP*
35	**Rybnikov A.**	PhD st	ECAL0	0,5	LNP
36	Rymbekova A.	PhD st	Data analysis	0,1	LNP
37	**Savin I.**	scient	Scien. team leader, data analysis	0,5	LHEP
38	Salmina E.	PhD st	Data analysis	1,0	LHEP*
39	Samartsev A.	tech	designer	0,5	LNP
40	**Selyunin A.**	PhD st	HCAL1, ECAL0	0,5	LNP
41	**Slunechka M.**	scient	Data taking	1,0	LNP
42	Smirnov G.	scient	Data analysis	0,1	LHEP
43	Tokmenin V.	tech	MW1	0,5	LNP
44	Fedoseev D.	tech	ECAL0	0,5	LNP
45	**Frolov V.**	scient	DAQ, ECAL0	1,0	LNP
46	Tchalyshev V.	tech	ECAL0	0,5	LNP
47	Chirikov-Zorin I.	scient	ECAL0	0,8	LNP
48	Yukaev A.	tech	HCAL1	0,5	LHEP
49	Janata A.	scient	Data taking	1,0	LNP

7. TIMELINES OF THE PROJECT

2017:
- Participation in COMPASS data taking (see chapter 2.7);
- Maintenance during running of MW1, HCAL1 and ECAL0 (see chapter 2.4-2.6);
- Development/support of MW1/HCAL1/ECAL0 software;
- Temporary decommissioning of ECAL0;
- Analysis of COMPASS experimental data;

2018:
- Participation in COMPASS data taking;
- Maintenance during running of MW1, HCAL1;
- Development/support of MW1/HCAL1 software;
- Analysis of COMPASS experimental data;

2019:
- Temporary decommissioning of MW1/HCAL1;
- Analysis of COMPASS experimental data;

8. FINANCE PROFILE

The common JINR expenses for a project stage in 2014-2016 (theme 1085) were equal to 770 thousand US dollars. $130 thousand were allocated to CERN (NA58, COMPASS-II) for support of JINR experts in CERN. The collaboration of NA58 allocates 40 thousand Swiss francs a year for payment of the common works performed by JINR engineers in CERN during preparation and support of an experiment and data taking. In three years $25 thousand were spent from grants of the Czech Republic. Some recourses of theme 1085 were spent also for holding the international working meetings in Suzdal (May, 2015).

The sum of necessary financing on 2017 - 2019 is equal to 733 thousand US dollars from the JINR budget. The main part of these expenses is required for participation of JINR physicists in a COMPASS data taking, for maintenance of detectors and contribution to the common fund of collaboration according to obligations of MoU. The finance profile, presented in Table 7, includes the travel money for JINR physicists, contribution to the common COMPASS fund, expenses for maintenance of HCAL1, ECAL0 and MW1. The scheduled plan of work is given in Table 8.

TABLE 7: JINR finance profile for 2017-2019 (in K$)

#	Item	Total	2017	2018	2019
1.	design bureau (man-h)				
2.	workshops (man-h)				
3.	Materials	45	20	15	10
4.	Equipment	75	25	25	25
5.	Subcontracts (collab common fund)	222	72	75	75
6.	Travels, including outside RUSSIA inside RUSSIA	 376 15	 150 5	 130 5	 96 5
	Total K$	733	272	250	211

Table 8. Scheduled plan of works on the project

		Year											
№	Item	2017				2018				2019			
		I	II	III	IV	I	II	III	IV	I	II	III	IV
1	Data taking												
2	ECAL0 preparation												
3	HCAL1 preparation												
3	ECAL0 maintenance												
4	HCAL1 maintenance												
5	MW1 preparation												
6	MW1 maintenance												
7	MW1/HCAL1 software												
8	ECAL0 software												
9	Data analysis												

The resources allocated to materials and equipment equal to 45 thousand dollars for three year. Mostly these resources will be spent for reparation and modernization of the low-voltage power supply system of MW1, modernization and maintenance of modules of the electromagnetic calorimeter of ECAL0 (in particular - monitoring system) and for possible repair of hadron calorimeter of HCAL1. The funds allocated for the equipment will be used for upgrades of the computers and electronics for detectors. The preliminary detailed travel finance profiles for each year of the project are given in Tables 9-11. After 2017 data taking the decommissioning of ECAL0 will be performed, because this detector will not be used for DY 2018 run. After finish of COMPASS-II data takings, in beginning of 2019 the decommissioning of HCAL1 and MW1 will be also done.

Table 9: Travel finance profile for 2017

N	Activity	#man-months	Appox. Expenses, K$
1	Preparation for data taking (3 detectors)	3	14
2	Maintenance of detectors during data taking	14	63
3	Temporary decommissioning of ECAL0	2	9
3	International conferences and workshops	3	14
4	Participation in Collaboration meetings	3	13
5	Support of works on target maintenance, hall engineering, DAQ, data production and alignment	2	10
6	Participation in group meeting: analysis meeting, technical board, drafting committees and collaboration board	6	27

Table 10: Travel finance profile for 2018

N	Activity	#man-months	Appox. Expenses, K$
1	Preparation for data taking (2 detectors)	3	14
2	Maintenance of detectors during data taking	12	54
3	International conferences and workshops	3	14
4	Participation in Collaboration meetings	2	10
5	Support of works on target maintenance, hall engineering, DAQ, data production and alignment	2	10
6	Participation in group meeting: analysis meeting, technical board, drafting committees and collaboration board	6	28

Table 11: Travel finance profile for 2019

N	Activity	#man-months	Appox. Expenses, K$
1	Temporary decommissioning of detectors (2 detectors)	4	18
3	International conferences and workshops	6	28
4	Participation in Collaboration meetings	4	18
6	Participation in group meeting: analysis meeting, technical board, drafting committees and collaboration board	7	32

References

1. COMPASS Collaboration, F. Gautheron et al., SPSC-P-340, CERN-SPSC-2010-014, 2010.
2. COMPASS Collaboration, P.Abbon et al., NIMA 577 (2007) 455–518
3. COMPASS Collaboration, P.Abbon et al., NIMA 779 (2015) 69
4. Quintans C. (for COMPASS Collaboration) Drell-Yan physics at COMPASS, Proc of XXII Inter-national Workshop on Deep-Inelastic Scattering and Related Subjects, Warsaw, Poland, 28 April -2 May. 2014. 6 p.
5. Fuchey E. (for COMPASS Collaboration) GPD program at COMPASS, Proc of Conf «QCD Evolution 2015». Jefferson Lab (JLAB). Newport News Virginia. USA. 26-30 May. 2015. 9 p.
6. E. Iarocci, Nucl. Instr. and Meth. 217 (1983) 30.
7. W. Busza, Nucl. Instr. and Meth. A 265 (1988) 210.
8. V. M. Abazov, et al., preprint JINR P13-2003-198, Dubna (2003) .
9. V. M. Abazov, et al., preprint JINR P13-2004-155, Dubna (2004) .
10. N. V. Vlasov, et al., Instruments and Experimental Techniques 49 (2006) 41.
11. Gasser J., Ivanov M. A., Sainio M. E. Revisiting at low energies, Nuclear Physics B. 2006. V. 745 P. 84-108.
12. Adolph C. et al. (COMPASS Collaboration) Measurement of the Charged-Pion Polarizability , Phys. Rev. Lett. 2015. V. 114. P. 062002
13. C. Patrignani et al. (Particle Data Group), Chin. Phys. C, 40, 100001 (2016).
14. Adolph C. et al. (COMPASS Collaboration), Search for exclusive photoproduction of Zc± (3900) atCOMPASS, Phys. Lett. B. 2015. V. 742. P. 330
15. Dutta D. et al. Pion-induced Drell-Yan processes and the flavor-dependent EMC effect, Phys. Rev. C. 2011. V. 83. P. 042201
16. "First measurement of the transverse spin asymmetries of the deuteron in semi-inclusive deep inelastic scattering", PRL 94 (2005) 202002
17. "Gluon polarization in the nucleon from quasi-real photoproduction of high-pT hadron pairs", PLB 633 (2006) 25–32
18. John P. Ralston and Davison E. Soper, Nucl. Phys., B152, 109, 1979.
19. R. D. Tangerman and P. J. Mulders, Phys. Rev., vol. D51, 3357–3372, 1995.
20. Daniel Boer and P. J. Mulders, Phys. Rev., D57, 5780–5786, 1998.
21. Stanley J. Brodsky, Dae Sung Hwang and Ivan Schmidt, Phys. Lett., B530, 99–107, 2002.
22. John C. Collins,Phys. Lett., B536, 43–48, 2002.
23. X.D. Ji and F. Yuan, Phys. Lett., B543, 66–72, 2002.
24. Andrei V. Belitsky, X. Ji and F. Yuan, Nucl. Phys., B656, 165–198, 2003.
25. Daniel Boer, P. J. Mulders and F. Pijlman, Nucl. Phys., B667, 201–241, 2003.
26. U. D'Alesio and F. Murgia, Prog.Part.Nucl.Phys., 61, 394–454, 2008.
27..M. Burkardt, C.A. Miller and W.D. Nowak, Rept.Prog.Phys., 73, 016201, 2010.
28. Vincenzo Barone, Franco Bradamante and Anna Martin,Prog.Part.Nucl.Phys.,65,267–333, 2010.
29. Dieter Mueller, D. Robaschik, B. Geyer, F. M. Dittes and J. Horejsi, Fortschr. Phys., 42, 101, 1994.
30. Xiang-Dong Ji, Phys. Rev., D55, 7114–7125, 1997.
31. A. V. Radyushkin, Phys. Lett., B449, 81–88, 1999.
32. C. Lorce and B. Pasquini, Phys.Rev., D84, 014015, 2011.
33. Cedric Lorce and Barbara Pasquini, Quark phase-space distributions and orbital angular momentum. 2012.
34. Xiangdong Ji, Xiaonu Xiong and Feng Yuan, Phys.Rev.Lett.,109, 152005, 2012.
35. Yoshitaka Hatta, Phys.Lett., B708, 186–190, 2012.
36. Cedric Lorce, Barbara Pasquini, Xiaonu Xiong and Feng Yuan, Phys.Rev., D85, 114006, 2012.
37. X.D. Ji, J.P. Ma and F. Yuan, Phys. Rev., D71, 034005, 2005.
38. John C. Collins and Andreas Metz, Phys. Rev. Lett., 93, 252001, 2004.
39. John Collins. Foundations of perturbative QCD. 2011
40. S. Mert Aybat and Ted C. Rogers, Phys.Rev., D83, 114042, 2011.
41. S. Mert Aybat, John C. Collins, Jian-Wei Qiu and Ted C. Rogers, Phys.Rev., D85, 034043, 2012.
42. X.¬D. Ji. Phys. Rev. Lett. 78 (1997) 610.

43. D. Boer et al., Phys. Rev. D57 (1998) 5780
44. R. N. Cahn, Phys. Lett. B78 (1978) 269
45. Guerrero F., Prades J. Kaon Polarizabilities in Chiral Perturbation Theory, Phys. Lett. B. 1997. V. 405. P. 341-346.
46. Ivanov M. A., Mizutani T. Pion and kaon polarizabilities in the quark confinement model, Phys. Rev. D. 1992. V. 45, P. 1580.
47. Terentev M. V. Structure of observable amplitudes for photon - 'soft' pion interaction, Sov. J. Nucl. Phys. 1972. V. 15. P. 665-674
48. Kaiser N. et al. Cross sections for low-energy $\pi - \gamma$ reactions, Eur. Phys. J. A. 2008. V. 36.
49. Adolph C. et al. (COMPASS Collaboration) First Measurement of Chiral Dynamics in $\pi-\gamma \to \pi-\pi-\pi+$, Phys. Rev. Lett. 2012. V. 108. P. 192001
50. Wang Q., Liu X.-H., Zhao Q. Photoproduction of hidden charm pentaquark states Pc+ (4380) and Pc+ (4450), Phys. Rev. D. 2015. V. 92. P. 034022
51. Karliner M., Rosner J. L. Photoproduction of exotic baryon resonances, Phys. Lett. B. 2016. V. 752. P. 329-332.
52. Dutta D. et al. Pion-induced Drell-Yan processes and the flavor-dependent EMC effect, Phys. Rev. C. 2011. V. 83. P. 042201
53. Huang Y. et al. Pion-induced production of the Zc (3900) off a nuclear target, Phys. Rev. D. 2016. V. 93. P. 034022
54. «Measurement of azimuthal hadron asymmetries in semi-inclusive deep inelastic scattering off unpolarised nucleons», NPB 886 (2014) 1046
55. Measurement of the charged-pion polarisability»,PRL 114 (2015) 062002
56. «Multiplicities of charged pions and unidentified charged hadrons from deep-inelastic scattering of muons off an isoscalar target», CERN-EP/2016-095, accepted by PLB
57. HERMES Collaboration, A. Airapetian, et al., Phys. Rev. D 87 (2013) 074029.
58. EMC, J. Ashman, et al., Z. Phys. C 52 (1991) 361.

Appendix: The list of the COMPASS publications
(updated on March 27, 2017).

1."Measurement of the spin structure of the deuteron in the DIS region", PLB 612 (2005) 154
2. "First measurement of the transverse spin asymmetries of the deuteron in semi-inclusive deep inelastic scattering", PRL 94 (2005) 202002
3. "Search for the Φ(1860) pentaquark at COMPASS", EPJ C41 (2005) 469–474
4. "Gluon polarization in the nucleon from quasi-real photoproduction of high-p_T hadron pairs", PLB 633 (2006) 25–32
5."The Deuteron Spin-dependent Structure Function g1d and its First Moment", PLB 647 (2007) 8–17
6."A new measurement of the Collins and Sivers asymmetries on a transversely polarised deuteron", NP B765 (2007) 31–70
7."The Compass Experiment at CERN", NIMA 577 (2007) 455–518
8."Spin asymmetry A1d and the spin-dependent structure function g_1^d of the deuteron at low values of x and Q^2",PLB 647 (2007) 330–340
9."Double spin asymmetry in exclusive ρ^0 muon-production at COMPASS", EPJ C52 (2007) 255–265
10."The Polarised Valence Quark Distribution from semi-inclusive DIS", PLB 660 (2008) 458–465
11."Collins and Sivers asymmetries for pions and kaons in muon-deuteron DIS", PLB 673 (2009), 127–135
12."Direct Measurement of the Gluon Polarisation in the Nucleon via Charm Meson Production", CERN-PH-EP/2008-003
13."Gluon Polarisation in the Nucleon and Longitudinal Double Spin Asymmetries from Open Charm Muon production", PLB 676 (2009) 31–38
14."Flavour Separation of Helicity Distributions from Deep Inelastic Muon-Deuteron Scattering", PLB 680 (2009) 217–224
15."Measurement of the Longitudinal Spin Transfer to Λ and anti-Λ Hyperons in Polarized Muon DIS", EPJC 64 (2009) 171–179
16."Observation of a $J^{PC} = 1^{-+}$ exotic resonance in diffractive dissociation of 190 GeV/c π– into π–π–π+",PRL 104 (2010) 241803
17."The spin-dependent structure function of the proton g1p and a Test of the Bjorken Sum Rule", PLB 690 (2010) 466–472
18."Measurement of the Collins and Sivers asymmetries on transversely polarised protons", PLB 692 (2010) 240–246
19."Azimuthal asymmetries of charged hadrons produced by high energy muons off longitudinally polarized deuterons", EPJC 70 (2010) 39–49
20."Quark Helicity Distributions from Longitudinal Spin Asymmetries in Muon-Proton and Muon-Deuteron Scattering", PLB 693 (2010) 227–235
21."First Measurement of Chiral Dynamics in $\pi-\gamma \rightarrow \pi-\pi-\pi+$ ", PRL 108 (2012) 192001
22."Leading order determination of the gluon polarisation from DIS events with high-p_T hadron pairs", PLB 718 (2013) 922
23."Transverse spin effects in hadron-pair production from semi-inclusive deep inelastic scattering", PLB 713 (2012) 10
24."Experimental investigation of transverse spin asymmetries in muon-p SIDIS processes: Collins asymmetries", PLB 717 (2012) 376
25."Experimental investigation of transverse spin asymmetries in muon-p SIDIS processes: Sivers asymmetries", PLB 717 (2012) 383
26."Measurement of the Cross Section for High-pT Hadron Production in Scattering of 160 GeV/c Muons off Nucleons" , PRD 88(2013)
27."Exclusive ρ^0 muoproduction on transversely polarised protons and deuterons", NPB 865 (2012) 1
28."D* and D Meson Production in Muon-Nucleon Interactions at 160 GeV/c", EPJC 72 (2012) 2253

29."Leading and Next-to-Leading Order Gluon Polarisation in the Nucleon and Longitudinal Double Spin Asymmetries from Open Charm Munoproduction", PRD 87 (2013)

30. «Study of Σ(1385) and Ξ(1321) hyperon and antihyperon production in deep inelastic scattering», EPJC 73 (2013) 2581.
31. «Hadron transverse momentum distributions in muon deep inelastic scattering at 160 GeV/c», EPJC 73 (2013) 2531.
32. «Erratum: Hadron transverse momentum distributions in muon deep inelastic scattering at 160 GeV/c», EPJC 75 (2015) 94
33. «Transverse target spin asymmetries in exclusive ρ0 muoproduction», PLB B731 (2014) 19
34. «Measurement of azimuthal hadron asymmetries in semi-inclusive deep inelastic scattering off unpolarized nucleons», NPB (2014) 1046
35. «A high statistics measurement of transverse spin effects in dihadron production from muon-proton semi-inclusive deep-inelastic scattering», PLB 736 (2014) 124
36. «Measurement of radiative widths of a_2(1320) and π2(1670)», EPJA 50 (2014) 79
37.»Spin alignment and violation of the OZI rule in exclusive ω and φ production in pp collisions», NPB 886 (2014) 1078
38. «Measurement of the charged-pion polarisability», PRL 114 (2015) 062002
39. «Search for exclusive photoproduction of Z±c (3900) at COMPASS», PLB 742 (2015) 330
40. «Odd and Even Partial Waves of ηπ− and η'π− in π−→ η(')π−p at 191 GeV/c», PLB 740 (2015)
41. «Collins and Sivers asymmetries in muonproduction of pions and kaons off transversely polarised proton», PLB 744 (2015) 250
42. «The COMPASS setup for physics with hadron beams», NIMA 779 (2015) 69
43. «Observation of a new narrow axial-vector meson a1(1420)», PRL 115 (2015) 082001
44. «The spin structure function g1 p of the proton and a test of the Bjorken sum rule», PLB 753 (2016) 18
45. «Interplay among transversity induced asymmetries in hadron leptoproduction», PLB 753 (2016) 406
46. «Resonance Production and ππ S-wave in π−+p→π−π−π++precoil at 190 GeV/c», PDR 95 (2017)
47. «Longitudinal double spin asymmetries in single hadron quasi-real photoproduction at high pT», PLB 753 (2016) 573
48. «Leading-order determination of the gluon polarisation using a novel method», CERN-PH-EP-2015-328, accepted EPJC
49. «Multiplicities of charged pions and unidentified charged hadrons from deep-inelastic scattering of muons off an isoscalar target», PLB 764 (2017) 001
50. «Exclusive ω meson muoproduction on transversely polarised protons», CERN-EP/2016-157, NPB 915 (2017) 454
51. «Multiplicities of charged kaons from deep-inelastic muon scattering off an isoscalar target», PLB 767 (2017) 113
52. «Azimuthal asymmetries of charged hadrons produced in high-energy muon scattering off longitudinally polarised deuterons», CERN-EP/2016-245, submitted EPJC
53. «Sivers asymmetry extracted in SIDIS at the hard scale of the Drell-Yan process at COMPASS», CERN-EP/2016-250, submitted PLB
54. «Final COMPASS results on the deuteron spin-dependent structure function g1d and the Bjorken sum rule», CERN-EP/2016-299, accepted PLB
55. «First measurement of the Sivers asymmetry for gluons from SIDIS data», CERN-EP/2017-003, accepted PLB

COMPASS results included in the meson tables of the latest version of the PDG are:

* the radiative width of the $a_2(1320)$ and $\pi_2(1670)$ from 2004 data
(EPJA 50 (2014) 79):
http://pdg.lbl.gov/2016/
http://pdg.lbl.gov/2016/

* mass and width of the $a_4(2040)$ and $a_2(1320)$ (though the latter is omitted from the PDG average) and their ratios of the branchings into $\pi\,\eta'/\pi\,\eta$
(PLB 740 (2015) 303):
http://pdg.lbl.gov/2016/
http://pdg.lbl.gov/2016/

* mass and width of the novel $a_1(1420)$ from the 3π letter
(PRL 115 (2015) 082001):
http://pdg.lbl.gov/2016/

* non-observation of the X(3900) (PLB 742 (2015) 330):
http://pdg.lbl.gov/2016/

Form 26

Schedule proposal and resources required for the implementation of the Project

COMPASS-II

Expenditures, resources, financing sources			Costs (k$) Resource requirements	Proposals of the Laboratory on the distribution of finances and resources		
				1st year	2nd year	3rd year
Expenditures		Main units of equipment, work towards its upgrade, adjustment etc.				
		Construction/repair of premises				
		Materials				
Required resources	Standard hour	Resources of – Laboratory design bureau; – JINR Experimental Workshop; – Laboratory experimental facilities division; – accelerator; – computer.				
		Operating costs.	222	72	75	75
Financing sources	Budgetary resources	Budget expenditures including foreign-currency resources.	733	272	250	211
	External resources	Contributions by collaborators.	90	30	30	30
		Grants.	24	8	8	8
		Contributions by sponsors.				
		Contracts.				
		Other financial resources, etc.				

PROJECT LEADER

Форма № 26

Предлагаемый план-график и необходимые ресурсы для осуществления проекта_____COMPASS-II_____

Наименования затрат, ресурсов, источников финансирования			Стоимость (тыс. долл.). Потреб-ности в ресурсах	Предложение лаборатории по распределению финансирования и ресурсов		
				1 год	2 год	3 год
Затраты		Основные узлы оборудования, работы по его обновлению, наладке и т.п.				
		Строительство/ремонт помещений				
		Материалы				
Необходимые ресурсы	Нормо-час	Ресурсы – конструкторского бюро лаборатории, – опытного производства ОИЯИ, – опытного производства лаборатории, – ускорителя, – реактора, – ЭВМ.				
		Эксплуатационные расходы	222	72	75	75
Источники финансирования	Бюджетные средства	Затраты из бюджета, в том числе инвалютные средства	733	272	250	211
	Внебюджетные средства	Вклады коллаборантов.	90	30	30	30
		Средства по грантам.	24	8	8	8
		Вклады спонсоров.				
		Средства по договорам.				
		Другие источники финансирования и т.д.				

РУКОВОДИТЕЛЬ ПРОЕКТА

Form 29

Estimated expenditures for the Project COMPASS-II

	Expenditure items	Full cost	1st year	2nd year	3rd year…
	Direct expenses for the Project				
1.	**Accelerator, reactor**	**h**			
2.	**Computers**	**h**			
3.	**Computer connection**	**k$**			
4.	**Design bureau**	**standard hour**			
5.	**Experimental Workshop**	**standard hour**			
6.	**Materials**	**k$**	**20**	**15**	**10**
7.	**Equipment**	**k$**	**25**	**25**	**25**
8.	**Construction/repair of premises**	**k$**			
9.	**Payments for agreement-based research**	**k$**			
10.	**Travel allowance, including:**	**k$**			
	a) non-rouble zone countries		**150**	**130**	**96**
	b) rouble zone countries		**5**	**5**	**5**
	c) protocol-based		**72**	**75**	**75**
	Total direct expenses	**733**	**272**	**250**	**211**

PROJECT LEADER

LABORATORY DIRECTOR

LABORATORY CHIEF ENGINEER-ECONOMIST

Форма № 29

Смета затрат по проекту COMPASS-II

NN пп	Наименование статей затрат	Полная стоимость	1 год	2 год	3 год
	Прямые расходы на Проект				
1.	Ускоритель, реактор	час.			
2.	ЭВМ	час.			
3.	Компьютерная связь	тыс. долл.			
4.	Конструкторское бюро	нормо-час			
5.	Опытное производство	нормо-час			
6.	Материалы	тыс. долл.	20	15	10
7.	Оборудование	тыс. долл.	25	25	25
8.	Строительство/ремонт помещений	тыс. долл.			
9.	Оплата НИР, выполняемых по договорам	тыс. долл.			
10.	Командировочные расходы, в т.ч.	тыс. долл.			
	а) в страны нерублевой зоны		150	130	96
	б) в города стран рублевой зоны		5	5	5
	в) по протоколам		72	75	75
	Итого по прямым расходам:	733	272	250	211

РУКОВОДИТЕЛЬ ПРОЕКТА

ДИРЕКТОР ЛАБОРАТОРИИ

ВЕДУЩИЙ ИНЖЕНЕР-ЭКОНОМИСТ ЛАБОРАТОРИИ